SR 90

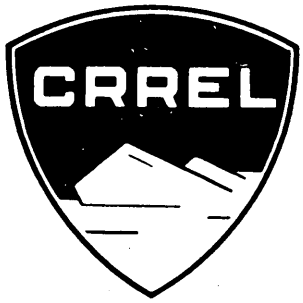

Special Report 90

AN INVESTIGATION OF MASS TRANSFER BY SUBLIMATION FROM A SNOW-SURFACE

by

Clement B. Edgar, Jr.

SEPTEMBER 1966

U.S. ARMY MATERIEL COMMAND
COLD REGIONS RESEARCH & ENGINEERING LABORATORY
HANOVER, NEW HAMPSHIRE

Distribution of this document is unlimited

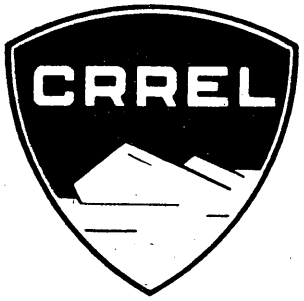

Special Report 90

AN INVESTIGATION OF MASS TRANSFER BY SUBLIMATION FROM A SNOW-SURFACE

by

Clement B. Edgar, Jr.

SEPTEMBER 1966

U.S. ARMY MATERIEL COMMAND
COLD REGIONS RESEARCH & ENGINEERING LABORATORY
HANOVER, NEW HAMPSHIRE

DA-AMC-27-021-63-G1
Dartmouth College

SUMMARY

The problem of mass transfer by sublimation from a snow surface subjected to radiation and forced convection is investigated. The effect of irradiation from a nonisothermal source on the mass transfer rate is studied. Forced convection of the "flat plate" and "entrance region" type is investigated. Entrance effects are seen to have a negligible influence on the mass transfer rate. The effect of the nonisothermal snow surface is shown to be negligible. A thermal network analysis is developed to predict the mass transfer rate due to the combined effects of radiation and forced convection.

Experimental results for mass transfer from a snow surface in the entrance region of a rectangular duct show good agreement with the predicted mass transfer rate.

AN INVESTIGATION OF MASS TRANSFER BY SUBLIMATION FROM A SNOW-SURFACE

by

Clement B. Edgar, Jr.

INTRODUCTION

One of the chief maintenance problems in an undersnow camp, such as Camp Century, Greenland, is the continuous closure of the tunnels. This is brought about by a densification of the snow layer and a plastic flow or "creep" of the snow-walls. The combined effects of plastic flow and densification tend to close the tunnels at rates of about 1 ft per year*. Sublimation and subsequent mass transfer of the snow walls has been suggested as a means of control [R. Waterhouse, Personal Communication].

A study was begun in June 1963 by W. D. Lamb and the author to determine the significant environmental factors which influence the mass transfer rate and to develop an analysis for predicting the rate. An order of magnitude analysis was made; it was found that sufficient mass transfer rates could be attained provided a suitable method of putting the energy into the snow surface was available. Lamb subsequently reported on the feasibility of several methods (Lamb, 1964). The method studied in this paper is irradiation of the snow surface, although the analysis applies for other methods as well.

As snow removal by vapor transfer has been shown to be feasible, it was desired to develop an adequate analysis for determining mass transfer rates. Also the quantitative influence of nonisothermal irradiation, convection from the nonisothermal snow surface, snow surface roughness, and the entrance region on the rate of mass transfer was not known. This investigation has produced an adequate analysis for predicting mass transfer rates and has also determined the importance of these factors.

Camp Century (Fig. 1) is a U.S. Army undersnow camp located on the Greenland Ice Cap. The side trenches containing the buildings are approximately 400 ft long, 24 ft wide, and 16 ft high. The smaller buildings are approximately 76 ft long, 16 ft wide and 12 ft high. This left a 3 to 4-ft spacing between the sides of the building and the snow tunnel.

The scheme for producing mass transfer is to supply energy to the snow surface; this energy raises the snow surface temperature and sublimes the snow. The air immediately adjacent to the snow surface is saturated with vapor. Air is forced through the tunnels at low velocities (less than 15 ft/sec) to carry off the vapor.

As the air first enters the tunnel, it contains a quantity of moisture depending on its dewpoint temperature (the moisture content may be determined from psychrometric tables). The vapor from the heated snow surface is transferred into the air and the moisture content is subsequently increased as the air proceeds down the tunnel. Air layers near the surface contain more moisture than those further away and thus a vapor gradient is established at the surface. The region near the surface where the vapor gradient is significant

---

*Field data taken by the Cold Regions Research and Engineering Laboratory (CRREL), U.S. Army Materiel Command, Hanover, N.H. (1961-1963).

is called the "boundary layer." As the air proceeds down the tunnel, the vapor gradient extends further out from the surface and thus the boundary layer "develops" or increases in thickness from the entrance. It is shown in Appendix D that the boundary layer thickness is given by the equation:

$$\delta = 0.382\, x \left(\frac{Vx}{\nu}\right)^{-1/5}$$

where x is the distance from the entrance (ft), V is the velocity of the air (ft/hr) and ν is the kinematic viscosity of the air (ν = 0.463 ft^2 /hr at 0F). On the basis of this equation, we may compute the boundary layer thickness for several distances from the entrance:

	V = 5 ft/sec	V = 10 ft/sec
x [ft]	δ [ft]	δ [ft]
25	0.61	0.53
50	1.06	0.92
100	1.84	1.60
200	3.20	2.78

From the above table it is seen that, even for a tunnel 200 ft long the boundary layer thickness is less than the 4-ft distance between the side of the building and the snow wall. Thus the forced convection heat and mass transfer is of the "entrance region" type; it occurs in a developing boundary layer at the snow surface that has not yet filled the passage width. Fully developed flow (where the boundary layer fills the space between the snow wall and the building) does not occur for about 300 to 400 ft.

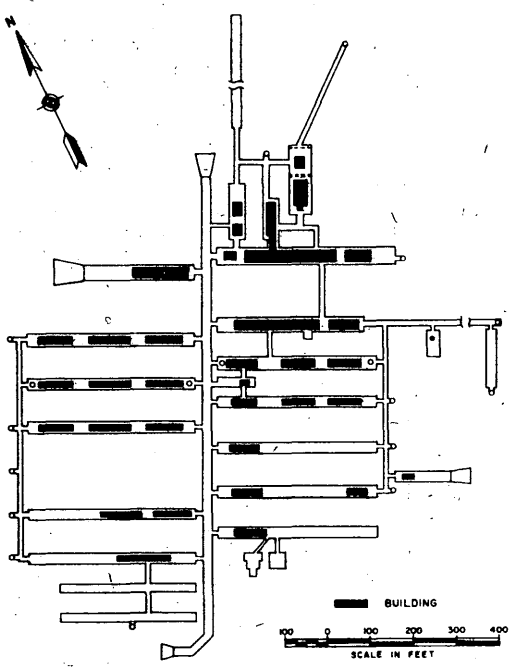

Figure 1. Diagram of Camp Century.

The convection heat and mass transfer in the snow tunnel should be investigated using a model which has geometric and dynamic similarity to the snow tunnel. Since snow tunnels are likely to have irregularities in cross section, geometric similarity between the tunnel and the model can only be approximated. The snow tunnel cross section is approximately rectangular, so the passage between the building side wall and the snow surface is essentially a rectangular passage with a height to width ratio of about 4 to 1 (building height 12 ft; distance between the building and snow wall 3 ft). The snow surface will be assumed to be irradiated by heaters fixed to the building wall. Hence the model

best representing the conditions in the snow tunnel is a rectangular duct with a snow floor and heated roof as shown below.

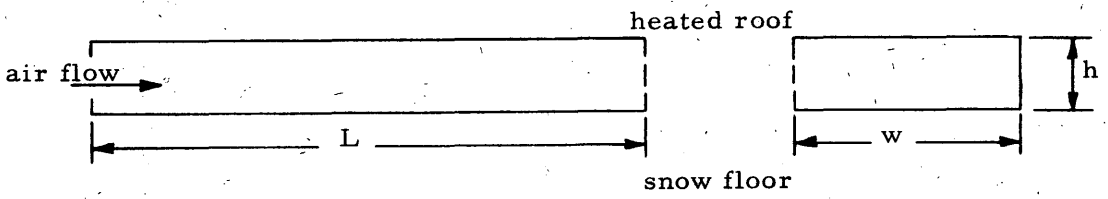

$h/w = 0.25$

$h/L = 0.05$

Since the flow situation in the tunnel is likely to be relatively complex (high level of turbulence, vortices, etc.), dynamic similarity between the tunnel and the model can likewise only be approximated. The important consideration is to make the model exhibit the entrance region flow as does the snow tunnel. This can be done by making the Reynolds number, based on the distance from the entrance ($Re_x = \frac{Vx}{\nu}$), approximately the same in both cases. This assures that the ratio of the boundary layer thickness δ to the distance from the entrance x is approximately the same for the snow tunnel and the rectangular duct.

The representation is completed by requiring the air temperature T_a and air dewpoint temperature T_{dp} to be the same for the snow tunnel and the flat duct. The air temperature is in the range -20F to +20F with the dewpoint slightly lower, from about -30F to +15F. The heating panel in the flat duct is assumed to be a uniform power source, but the analysis is applicable to other radiation sources as well. Excessive losses by conduction through the sides of the duct are eliminated in this investigation by adequate insulation, but the analysis is also capable of taking these losses into account.

The analysis will be applied to the simplified model described above, but it is able to account for complicating factors which may occur in practice. Constant reference to the practical situation will be made in the following sections and methods for taking the various complicating factors into account will be indicated.

NOMENCLATURE

Symbols	Units
A - Area	ft^2
e - Emissive power	$\frac{Btu}{hr}$
c_p - Specific heat at constant pressure	$\frac{Btu}{lb_m\text{-}F}$
D - Diffusion coefficient	ft^2/hr
F_{ij} - Radiation configuration factor from surface i to surface j	
g - Mass transfer of water vapor	$\frac{lb_m}{hr}$
h - Height of duct	ft

h_c - Forced convection heat transfer coefficient	$\frac{Btu}{hr\text{-}ft^2\text{-}F}$
h_D - Forced convection mass transfer coefficient	$\frac{ft}{hr}$
h_m - Sublimation heat transfer coefficient	$\frac{Btu}{hr\text{-}ft^2\text{-}F}$
h_r - Radiation heat transfer coefficient	$\frac{Btu}{hr\text{-}ft^2\text{-}F}$
H - Humidity ratio or specific humidity	$\frac{lb_w}{lb_a}$
H_a - Humidity ratio in free stream air	$\frac{lb_w}{lb_a}$
H_s - Humidity ratio at snow surface	$\frac{lb_w}{lb_a}$
H_w - Humidity ratio of air at an arbitrary surface	$\frac{lb_w}{lb_a}$
k - Coefficient of thermal conductivity	$Btu\text{-}ft\text{-}hr^{-1}ft^{-2}F^{-1}$
k_s - Mean surface protrusion	ft
L_s - Latent heat of sublimation for snow	$1220 \frac{Btu}{lb_m}$
P_i - Net heat transfer by radiation from zone i on the heating panel	$\frac{Btu}{hr\text{-}ft^2}$
q_c - Forced convection heat transfer	$\frac{Btu}{hr}$
q_m - Sublimation heat transfer	$\frac{Btu}{hr}$
q_r - Radiation heat transfer	$\frac{Btu}{hr}$
Q - Power output of heating panel	$\frac{Btu}{hr\text{-}ft^2}$
r - Radiant energy away from a surface	$\frac{Btu}{hr\text{-}ft^2}$
R_i - Net heat transfer by radiation to zone i on the snow surface	$\frac{Btu}{hr\text{-}ft^2}$
T - Temperature	°F
$\underline{T}$ - Absolute temperature	°R
T_a - Free stream air temperature	°F
T_{dp} - Free stream air dewpoint temperature	°F
T_s - Snow surface temperature	°F
T_p - Heating panel temperature	°F
T_w - Temperature of air at an arbitrary surface	°F
u - Irradiation of a surface	$\frac{Btu}{hr\text{-}ft^2}$

v_x - Boundary layer velocity, x direction — $\frac{ft}{hr}$

V - Free stream air velocity — $\frac{ft}{hr}$

V_o - Free stream air velocity upon entering the duct — $\frac{ft}{hr}$

x - Coordinate parallel to air flow — ft

y - Coordinate perpendicular to air flow — ft

α - Absorptivity

δ - Velocity boundary layer thickness — ft

δ' - Thermal boundary layer thickness — ft

δ'' - Humidity or vapor boundary layer thickness — ft

ϵ - Emissivity

μ - Dynamic viscosity — $lb_m/ft\text{-}hr$

ν - Kinematic viscosity — $\frac{ft^2}{hr}$

ρ - Air density — $\frac{lb_m}{ft^3}$

ρ - Reflectivity (section I)

σ - Stefan-Boltzmann constant — 1.713×10^{-9} Btu/hr-ft^2-R^4

τ_w - Shear stress — $\frac{lb_f}{ft^2}$

τ - Transmissivity

∞ - (subscript) - pertains to conditions at infinity before experiment

Dimensionless Groups

$\frac{C_f}{2}$ - Coefficient of skin friction — $\frac{\tau_w}{\rho V^2}$

St - Stanton number — $\frac{q_c/A}{\rho c_p V(T_w - T_\infty)}$

$\frac{h_D}{V}$ - Dimensionless mass transfer coefficient — $\frac{g/A}{\rho V(H_w - H_\infty)}$

Le - Lewis number = Sm/Pr — $\frac{k}{\rho c_p D}$

Pr - Prandtl number — $\frac{c_p \mu}{k}$

Re_x - Reynolds number — $\frac{Vx}{\nu}$

Sm - Schmidt number — $\frac{\mu}{\rho D}$

MASS TRANSFER BY SUBLIMATION FROM A SNOW-SURFACE

I. RADIATION TO THE SNOW SURFACE

The radiant energy emitted by any body is transmitted to the receiving bodies by electromagnetic waves of various wavelengths. Receiving bodies may absorb, reflect, or transmit the radiant energy. The fractions of incident energy absorbed, reflected, and transmitted are called the absorptivity α, reflectivity ρ, and transmissivity τ, respectively. By definition:

$$\alpha + \rho + \tau = 1 . \tag{1}$$

A blackbody is defined as one whose absorptivity is unity.

The absorptivity of the snow surface depends on the spectrum of radiation incident upon it. Radiation of the shorter wavelengths penetrates into the snow (i.e., the snow transmits the energy $\tau \neq 0$), while radiation of the longer wavelengths is almost entirely absorbed in the first few thousandths of an inch of the surface. Dorsey [1940] states that the absorptivity for ice is 0.966 and for frost 0.985 when the incident radiation is greater than 1 micron in wavelength. Since the heating panel will always be operated at temperatures below 200F, the radiation below 1 micron to the snow surface is entirely negligible.

The emissivities, ϵ_s and ϵ_p, (defined as the ratio of radiation emitted by the surface and the radiation emitted by a blackbody at the same temperature) of the snow surface and heating panel will be assumed equal to the absorptivities. It is well known that for small temperature differences (of the order of 100F), this assumption is valid.

The emissivity of the heating panel was measured with a radiometer (see Appendix A for a discussion of the experiment); it was determined to be 0.75.

The emissive power of a body is proportional to the product of its emissivity and the fourth power of its absolute temperature according to the Stefan-Boltzmann law:

$$\frac{e}{A} = \epsilon \sigma \underline{T}^4 \tag{2}$$

where σ is the Stefan-Boltzmann constant ($\sigma = 1.713 \times 10^{-9} \ \frac{\text{Btu}}{\text{hr-ft}^2\text{-R}^4}$).
The net transfer of energy by radiation between two bodies, however, is dependent upon the geometric configuration of the bodies as well as the emissivities. The relation must be of the form:

$$\frac{q_r}{A} = f(\epsilon_1, \epsilon_2, F_{12}) \sigma (\underline{T}_1^4 - \underline{T}_2^4) \tag{3}$$

$$0 < f(\epsilon_1, \epsilon_2, F_{12}) < 1$$

since the configuration and emissivities can only act to decrease the efficiency of radiation from the blackbody or ideal case.

Consider the radiant interchange between the directly opposed parallel plates shown below.

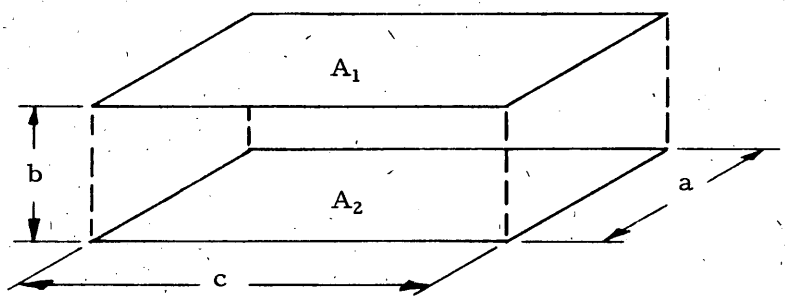

The radiation configuration factor F_{12} is defined as the fraction of radiation emitted by A_1 which is intercepted by A_2. The factor for this configuration is obtained by a four-way integration of Lambert's cosine relation; Hamilton and Morgan [1952] have performed this integration to obtain:

$$F_{12} = \frac{2}{\pi xy} \left\{ \ln \frac{(1+x^2)(1+y^2)^{1/2}}{1+x^2+y^2} + y\sqrt{1+x^2}\tan^{-1}\frac{y}{\sqrt{1+x^2}} + x\sqrt{1+y^2}\tan^{-1}\frac{x}{\sqrt{1+y^2}} - y\tan^{-1}y - x\tan^{-1}x \right\} \quad (4)$$

where $x = \frac{a}{b}$, $y = \frac{c}{b}$. If the areas A_1 and A_2 were black surfaces, the net heat transfer from A_1 to A_2 would be:

$$\frac{q_r}{A} = F_{12}\,\sigma(T_1^4 - T_2^4). \quad (5)$$

To account for the non-unit emissivities of A_1 and A_2, consider the diagram below:

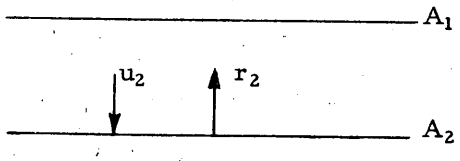

The quantity u_2 is the radiant energy transfer incident upon A_2; r_2 is the radiant energy transferred away from A_2. The quantity r_2 must be equal to the sum of the energies emitted and reflected from the surface since the amount transmitted in this case is certainly negligible:

$$r_2 = \rho_2 u_2 + \epsilon_2 \sigma T_2^4. \quad (6)$$

Combining with eq 1 gives:

$$r_2 = (1-\epsilon_2)u_2 + \epsilon_2 \sigma T_2^4. \quad (6a)$$

The net heat transfer by radiation from the surface A_2 is:

$$\frac{q_r}{A} = r_2 - u_2. \tag{7}$$

Combining eq 6a and 7, we obtain:

$$\frac{q_r}{A} = \frac{\epsilon_2}{1-\epsilon_2} (\sigma T_2^4 - r_2). \tag{8}$$

The quantities σT_2^4 and r_2 may be considered to be potentials separated by a conductance $\epsilon_2/1-\epsilon_2$ through which a current $\frac{q_r}{A}$ passes. Oppenheim [1956] has shown that eq 8 forms a basis for a network representation of heat transfer by radiation between gray ($\epsilon \neq 1$) surfaces. For the present case of directly opposed parallel plates, the network representation is:

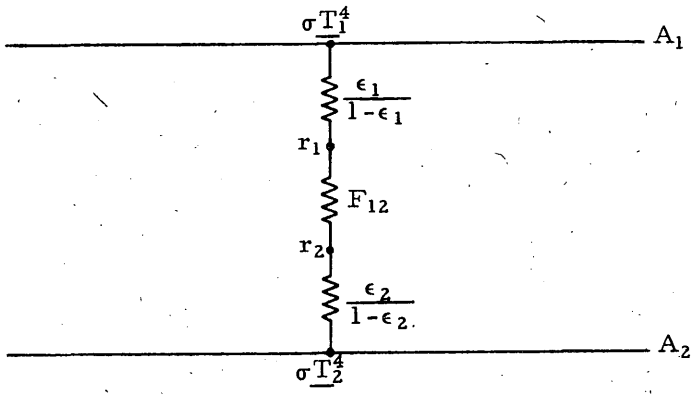

The network may be solved for the net heat transfer from A_1 to A_2:

$$\frac{q_r}{A} = \left[\frac{1}{\frac{1}{F_{12}} + \left(\frac{1}{\epsilon_1} - 1\right) + \left(\frac{1}{\epsilon_2} - 1\right)} \right] \sigma (T_1^4 - T_2^4). \tag{9}$$

For this case, the functional relationship indicated by eq 3 is given by the quantity in brackets on the right-hand side of eq 9. It should be noted that eq 3 to 9 apply only when the areas A_1 and A_2 are equal and must be modified for unequal areas [Oppenheim, 1956].

An approximate expression for the net heat transfer by radiation from the heating panel to the snow surface may be obtained by utilizing eq 9. The width of the heating panel is 20 in., the length 72 in., and the distance between the heating panel and the snow surface 5 in. The value for F_{12} is obtained from expression 4 with $x = 72/5$ and $y = 20/5$; this is $F_{12} = 0.738$. Using eq 9 with $\epsilon_1 = 0.75$ and $\epsilon_2 = 0.98$, we obtain:

$$\frac{q_r}{A} = 0.585\, \sigma(T_1^4 - T_2^4). \tag{10}$$

Equation 10 is likely to predict lower heat transfer rates in the center of the duct since the local configuration factor is larger than the average or total configuration factor calculated above. Since we are interested in predicting the mass transfer rate as a function of the distance from the duct entrance, we must consider the variation in configuration factor down the duct length. Further, eq 10 does not take into consideration the fact that sections along the snow surface have a nonisothermal source of radiant energy as the heating panel increases in temperature from the entrance of the duct.

To take these effects into account, the duct is divided into isothermal zones:

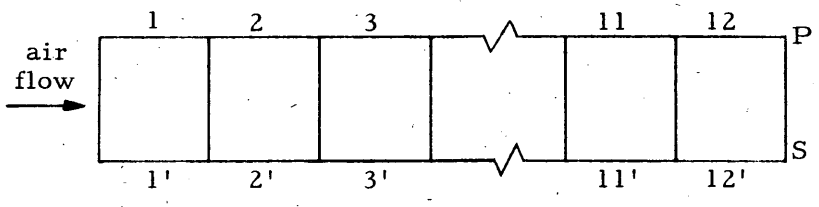

The network for this case is shown in part below.

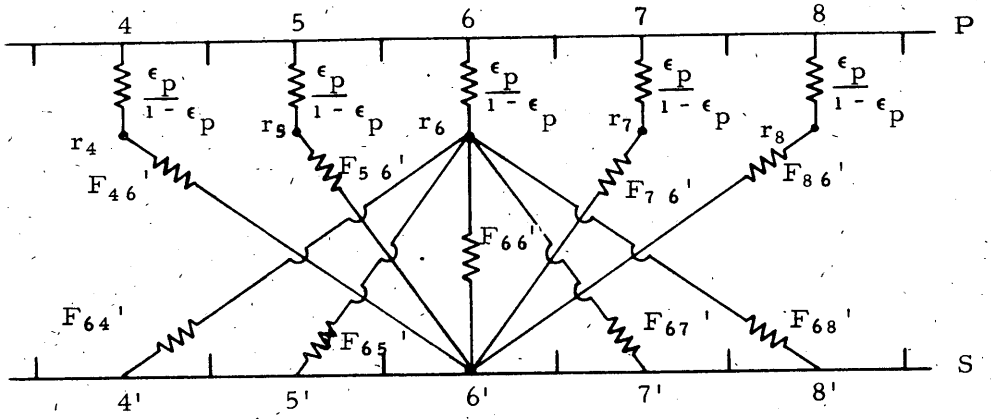

For the sake of simplicity all of the radiation paths (e.g., $(q_r/A)_{4-4'}$, $(q_r/A)_{5-7'}$, etc.) are not shown in this figure. The conductance $\epsilon_s/1-\epsilon_s$ is neglected since the snow surface is essentially a blackbody ($\epsilon_s = 0.98$, $\epsilon_s/1-\epsilon_s \gg 1$). The potentials r_1, r_2, etc. are calculated from the relation:

$$r_i = \frac{1}{\frac{\epsilon_p}{1-\epsilon_p} + \sum_{j=i-5}^{j=i+5} F_{ij}} \left[\frac{\epsilon_p}{1-\epsilon_p} \sigma \underline{T}_{pi}^4 + \sum_{j=i-5}^{j=i+5} F_{ij} \sigma \underline{T}_{sj}^4 \right] \quad (11)$$

which is derived in Appendix B. The configuration factors F_{ij} are also calculated in Appendix B.

Once the potentials r_i are known, the net heat transfer to a zone on the snow surface may be calulated from:

$$\left(\frac{q_r}{A}\right) = \sum_{j=i-5}^{i+5} F_{ij} \quad (r_j - \sigma T_{si}^4) . \qquad (12)$$

The net heat transfer from a zone on the heating panel is given by:

$$\left(\frac{q_r}{A}\right)_i = \sum_{j=i-5}^{i+5} F_{ij} \quad (r_i - \sigma T_{sj}^4). \qquad (13)$$

II. CONVECTION AND MASS TRANSFER

Energy is transferred from the snow surface by convection to a thin layer of air flowing over the surface. The mechanism for this energy transfer is responsible also for the momentum and the mass transferred to and from the surface respectively. A number of excellent references on this subject are available [Rohsenow and Choi, 1961; Schlichting, 1960; von Karman, 1921]; all the major derivations with the exception of Appendix E are taken from these sources and are considered to be well known.

The flow of any fluid, such as air or water, is disturbed at solid boundaries in such a manner as to slow the fluid particles near the walls of the boundaries. The region near the wall, where significant shearing forces act and the velocity is retarded, is called, following Prandtl, the "boundary layer." The region outside the boundary layer where the shear forces are negligible and the velocity is not significantly retarded is called the free stream.

If the fluid density is constant over the flow pattern, the flow is considered to be incompressible. The flow of air at low velocities (provided there are no large temperature gradients) can be considered to be incompressible. Further, the viscosity of air can be considered to be constant if there are no large temperature gradients (>50F across the boundary layer).

The flow may be either laminar or turbulent. A turbulent flow is characterized by random velocity fluctuations of the fluid particles. These fluctuations occur at high frequency and may be large or small depending on the flow situation. If the gross (or macro) flow pattern does not change with time, the flow is denoted steady. A steady turbulent flow is steady in the mean, or, equivalently, is one whose mean velocity at any point does not depend on time.

Any real flow pattern is three-dimensional; however, a given flow pattern may be considered to be two-dimensional or one-dimensional if changes in the fluid velocity occur significantly only in two directions or one direction, respectively.

The air flowing into the duct and over the snow surface is considered to be steady, two-dimensional, incompressible, turbulent flow. The momentum, heat, and mass transfer takes place in the boundary layer over the heating panel and the snow surface. To obtain the quantities of interest, the heat and mass transferred at the surface, in terms of the known quantities, surface temperature, air velocity, air temperature, and moisture content, one of two general approaches may be taken. The first is to write the momentum, energy, and mass conservation laws for the boundary layer in differential form and attempt to solve

the equations. The second is to require that the integrated or average momentum, energy, and mass be conserved over the height of the boundary layer. The latter method is known as the integral method and was first used by von Karman [1921]. This method is considerably simpler than the first, but the simplification results in a loss of information and more reliance must be placed on experimental and analytical work taken from other sources. A derivation of the momentum, energy, and mass integral equations for the boundary layer is given in Appendix C. For steady, two-dimensional, incompressible flow over the snow surface, the integral equations of momentum, energy and mass are:

Momentum:

$$\frac{C_f}{2} = \frac{1}{V}\frac{d}{dx}\int_0^{\delta} v_x\,dy - \frac{1}{V^2}\frac{d}{dx}\int_0^{\delta} v_x^2\,dy - \frac{\delta}{V}\frac{dV}{dx} \tag{14}$$

Energy:

$$St = \frac{1}{V}\frac{d}{dx}\int_0^{\delta'} v_x\,dy - \frac{1}{V}\frac{d}{dx}\int_0^{\delta'} \theta\, v_x\,dy \tag{15}$$

Mass:

$$\frac{h_D}{V} = \frac{1}{V}\frac{d}{dx}\int_0^{\delta''} v_x\,dy - \frac{1}{V}\frac{d}{dx}\int_0^{\delta''} \phi\, v_x\,dy\,. \tag{16}$$

The dimensionless numbers $\frac{C_f}{2}$, St, and $\frac{h_D}{V}$ are called the coefficient of skin friction, the Stanton number, and the dimensionless mass transfer coefficient. The quantities θ and ϕ are dimensionless temperature and humidity distributions ($\theta = \frac{T-T_s}{T_a-T_s}$, $\phi = \frac{H-H_s}{H_a-H_s}$).

Equations 15 and 16 exhibit a similarity independent of the momentum transfer in the boundary layer. If the thermal and humidity boundary layers coincide and the quantities θ and ϕ have the same y dependence, it follows that:

$$St = \frac{h_D}{V}\,. \tag{17}$$

This relation was modified by Chilton and Colburn [1934] to obtain a formula which agreed with their experiments:

$$St = \frac{h_D}{V}(Le)^{2/3} \tag{18}$$

where the Lewis number (Le) represents the ratio of thermal diffusion to mass diffusion in the boundary layer. For air, Le is approximately 0.857, so the correction is:

$$St = 0.902\,\frac{h_D}{V}\,. \tag{19}$$

Equation 14 is analogous to eq 15 and 16 if the variation of V is small and the term $\frac{dV}{dx}$ is negligible. If we assume that the velocity and thermal boundary layers coincide, we have:

$$\frac{C_f}{2} = St \quad . \tag{20}$$

This relation is due to Reynolds [Nikuradse, 1933] and is called the Reynolds analogy. This must be modified as was eq 17 to agree with experiment (Nikuradse, 1933; Schlichting, 1960):

$$St = \frac{C_f}{2} (Pr)^{-2/3} \quad . \tag{21}$$

The Prandtl number for air is approximately .70 and hence the correction becomes:

$$St = 1.27 \frac{C_f}{2} \quad . \tag{22}$$

Independent analyses proceeding from the differential equations of the boundary layer [Rohsenow and Choi, 1961; Schlichting, 1960; Shapiro, 1954] show that, as a necessary consequence of the equations of energy, mass, and momentum transfer in the boundary layer, the thermal, velocity, and humidity profiles must coincide when the turbulent Prandtl and Lewis numbers are unity. We would expect, then, that the corrections to the analogies 17 and 20 depend on these quantities and that they reduce to eq 17 and 20 when Le = Pr = 1. This is indeed the case as eq 18 and 21 indicate, and this has been well verified by experiment.

Equations 19 and 22 indicate that the dimensionless heat and mass transfer coefficients depend ultimately on the coefficient of skin friction or shear stress at the surface. The shear stress is dependent on free stream velocity, surface roughness, and the location of transition to turbulence in the boundary layer.

There are two types of turbulence to be considered in this problem. First, an environmental free turbulence level exists in the free stream air caused by disturbances in the air ordinarily found in the laboratory. Secondly, when non-turbulent air is drawn through the duct the boundary layer at the surface will be laminar at first and then turn turbulent because of instability caused by the wall. The turbulence generated in the boundary layer is called wall turbulence. The location of transition to turbulence in the boundary layer depends on the free stream turbulence level, surface roughness, and the air properties. Since, for this problem, the length of the laminar zone at the leading edge of the duct is so short, the boundary layer may be assumed to be turbulent from the leading edge.

The coefficient of skin friction is now dependent only on the air properties, air velocity, and the surface roughness of the snow. Skin friction coefficients for flat surfaces are usually taken from pipe flow data. von Karman [1921] first adapted the known semi-empirical relations for fully developed pipes to the flow over a semi-infinite flat plate. His method is presented in Appendix D.

The air just entering the duct is assumed to have uniform velocity as it enters. As stated above, shearing stresses tend to slow the air near the walls of the duct and form developing velocity profiles.

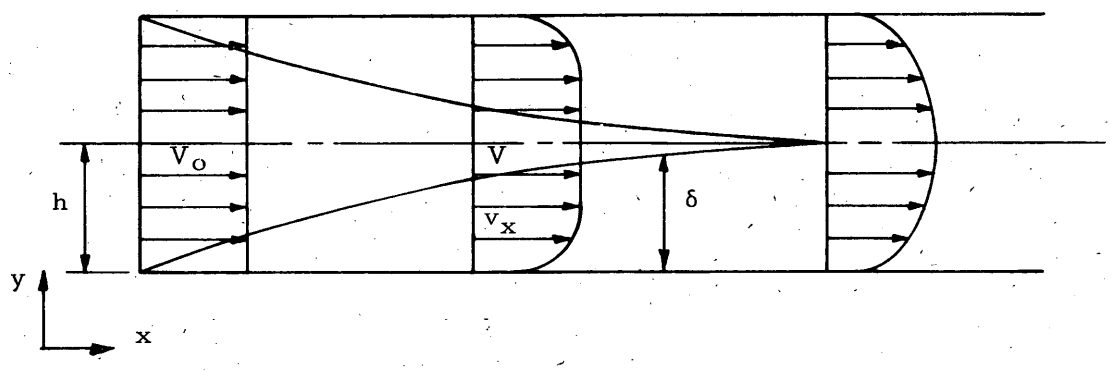

Continuity of flow requires that:

$$V_o h = \int_0^{\delta} v_x \, d_y + V(h - \delta) \quad . \tag{23}$$

As the boundary layer thickness, δ, increases in the x direction, continuity requires that the free stream velocity also increase. Thus the term $\frac{dV}{dx}$ is not zero and we would not expect the Reynolds analogy (eq 20 or 21) to hold. Furthermore, the relation for skin friction derived in Appendix D does not necessarily hold, since there the free stream velocity was assumed to be constant.

In Appendix E it is shown that the effect of accelerated free stream is negligible for turbulent flow in the entrance region. The shear stress expression derived for flow over a flat plate is, therefore, applicable to this case.

$$\frac{C_f}{2} = 0.0296 \left(\frac{Vx}{\nu}\right)^{-1/5} \tag{24}$$

This is usually referred to as the Blasius friction law for flat plates since it was adapted from the empirical friction law for pipes discovered by Blasius [1932]. Combining with eq 18 and 21 gives:

$$St = \frac{h_c}{\rho c_p V} = 0.0296 \left(\frac{Vx}{\nu}\right)^{-1/5} Pr^{-2/3} \tag{25a}$$

and

$$\frac{h_D}{V} = 0.0296 \left(\frac{Vx}{\nu}\right)^{-1/5} S_c^{-2/3} . \tag{25b}$$

One further assumption must be justified here. Since the power supplied to the heating panel is uniform, convection will cause an increasing temperature along the panel due to the decreasing heat transfer coefficient in the x direction. This will tend to heat the snow surface non-uniformly, causing an increasing snow surface temperature in the x direction. This effect is accentuated by the increasing radiation configuration factor as well as by the decreasing heat and mass transfer coefficients in the x direction. These factors invalidate the assumptions of constant humidity and constant temperature at the surface used in deriving the equation for shear stress in Appendix D. A method for analyzing the heat and mass transfer from a nonisothermal surface first used by Rubesin [1951] and later expanded by Tribus and Klein [1953] is presented in Appendix F. Nonisothermal effects are shown there to be entirely negligible for this problem.

Thus the relation derived in Appendix D for the shear stress is applicable here. The modified Reynolds analogies, eq 19 and 22, are used to calculate the heat and mass transfer coefficients.

III. SUBLIMATION OF SNOW BY A UNIFORM HEAT SOURCE

The nature of the problem posed thus far is so complex as to obscure some of the most interesting features of the sublimating snow surface. The radiation to the snow surface is dependent on the snow surface temperature as well as on the geometric configuration factor; this problem must be handled by a rather complicated numerical technique. Such a technique is presented later. In this section, however, the expressions for heat and mass transfer derived earlier will be used to analyze the problem of sublimation mass transfer from a flat plate of snow irradiated (or heated by some other means) by a uniform energy source. The energy flux will be independent of the snow surface temperature; this source might be a high temperature radiating surface or electrically heated wires embedded in the snow in such a way as to provide uniform power per unit of snow surface area [Lamb, 1964].

Flow of air over the snow will be assumed to be steady, two-dimensional, incompressible, and turbulent from the leading edge of the plate. Further, the air properties, density, viscosity, thermal conductivity, and specific heat will be assumed constant. Finally, the Reynolds number based on the distance from the leading edge of the plate is assumed low enough for the Blasius friction law and the 1/7 power profile to hold ($Re_x < 10^6$).

Once the above assumptions are made, the expressions for the heat and mass transfer coefficients may be taken directly as:

$$\frac{h_c}{\rho c_p V} = 0.0296 \left(\frac{Vx}{\nu}\right)^{-1/5} Pr^{-2/3} \qquad (25a)$$

$$\frac{h_D}{V} = 0.0296 \left(\frac{Vx}{\nu}\right)^{-1/5} Sm^{-2/3}. \qquad (25b)$$

For uniform power input to the snow surface Q, an energy balance yields:

$$Q = \frac{q_c}{A} + L_s \frac{g}{A}$$

$$= h_c (T_s - T_a) + L_s \rho h_D (H_s - H_a) . \qquad (26)$$

A sublimation mass transfer coefficient may be defined by the following equation:

$$L_s \frac{g}{A} = h_m (T_s - T_{dp}) \tag{27}$$

and from eq 26 it is apparent that:

$$h_m = L_s \rho h_D \frac{(H_s - H_a)}{(T_s - T_{dp})} \cdot \tag{28}$$

Using eq 26 and 27 and solving for the snow temperature one obtains:

$$T_s = \frac{Q + h_c T_a + h_m T_{dp}}{(h_c + h_m)} \cdot \tag{29}$$

From eq 24 and 25, we may write:

$$\rho h_D = \frac{h_c}{c_p} \left(\frac{Pr}{Sm}\right)^{2/3} = \frac{h_m}{L_s} \frac{(T_s - T_{dp})}{(H_s - H_a)} \cdot \tag{30}$$

Substituting these relations into eq 29, we have, after some rearrangements:

$$T_s - T_a = \frac{\frac{Q}{h_c} - (T_a - T_{dp}) \frac{\left(\frac{Pr}{Sm}\right)^{2/3}}{c_p} L_s \frac{H_s - H_a}{T_s - T_{dp}}}{1 + \frac{\left(\frac{Pr}{Sm}\right)^{2/3}}{c_p} L_s \frac{H_s - H_a}{T_s - T_{dp}}} \cdot \tag{31}$$

From this relation the snow temperature difference may be calculated for various values of the parameters $\frac{Q}{h_c}$, $(T_a - T_{dp})$, and the temperature level T_a. The results are presented in Appendix G. It is apparent that for values of $\frac{Q}{h_c}$ less than 10^{-2} the snow temperature remains at the wet bulb temperature of the air and the effect of heating on the snow surface temperature is negligible. It is also clear from these results that when the parameter $\frac{Q}{h_c}$ approaches 10^2, the snow temperature becomes higher than 32F.

The results may be utilized for engineering calculations in the following way:

1. The air velocity V, air temperature T_a, air dewpoint T_{dp}, and source strength Q are estimated.
2. The quantity $\frac{Q}{h_c}$ is determined using eq 24, and the temperature difference $T_a - T_{dp}$ is calculated.
3. The quantity $T_s - T_a$ is determined from the tables in Appendix G.

4. The mass transfer is calculated from the relation:

$$\frac{g}{A} = \rho h_D (H_s - H_a)$$

where h_D is found from eq 25 and the humidity ratios H_s and H_a are determined from psychrometric tables.

Relation 31 may be used to show that, for a given set of the parameters Q, V, and T_a, the dewpoint may be raised from a very low value to the air temperature, and the sublimation rate will at first decrease with x (distance from the leading edge), become almost uniform, then increase with x. This is due to the decreasing mass transfer coefficient being offset by the increasing snow temperature. The results of this calculation are also shown in Appendix G.

This is of great interest for the problem of snow removal, for it demonstrates that conditions in the snow tunnel affect not only the rate of mass transfer but also whether or not the rate is increasing or decreasing down the length of the tunnel.

IV. THERMAL NETWORK

A schematic diagram of the energy transfer in the duct is shown below:

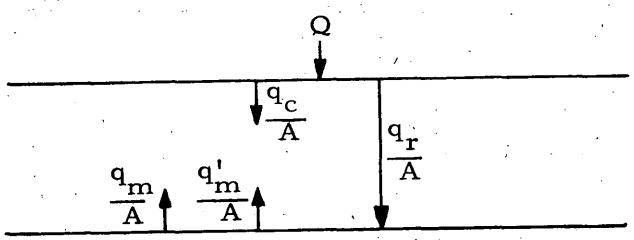

The power delivered to the heating panel per unit area Q is uniform. The heat transfer by radiation $\frac{q_r}{A}$, the heat transfer by convection $\frac{q_c}{A}$, and the mass transfer $\frac{g}{A}$ are functions of the distance from the edge of the duct.

A particularly convenient way of formulating the relatively complex energy transfer problem indicated here is the thermal network method used by Poppendiek and Tribus [1951]. The method consists of representing the

temperatures by potentials and the energy transfer coefficients by conductances. The constant energy source is represented by a current source:

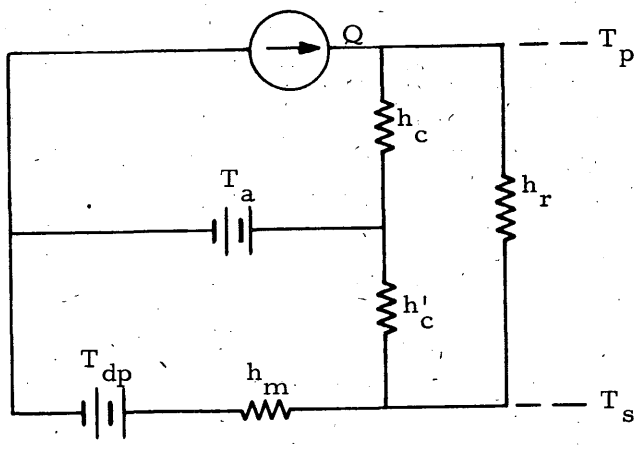

The thermal conductances are taken directly from sections I and II:

$$h_{r,T} = \frac{0.585\,\sigma\,(T_p^4 - T_s^4)}{(T_p - T_s)} \tag{32}$$

$$h_c = \rho c_p V (0.0376) \left(\frac{Vx}{\nu}\right)^{-1/5} \tag{33}$$

$$h_m = \frac{L_s h_c}{c_p} \left(\frac{Pr}{Sm}\right)^{2/3} \left(\frac{H_s - H_a}{T_s - T_{dp}}\right). \tag{34}$$

The network may be solved for the temperatures T_p and T_s by elementary circuit analysis (App. H). The results are:

$$T_s = \frac{(h_m T_{dp} + h'_c T_a)(h_r + h_c) + h_r(Q + h_c T_a)}{(h_r + h'_c + h_m)(h_r + h_c) - h_r^2} \tag{35}$$

$$T_p = \frac{(h_r + h'_c + h_m)(Q + h_c T_a) + h_r(h_m T_{dp} + h'_c T_a)}{(h_r + h'_c + h_m)(h_r + h_c) - h_r^2}. \tag{36}$$

Since the thermal conductances h_r and h_m are themselves functions of the unknown temperatures T_p and T_s, the system must be solved by iteration. The iteration scheme is to set the temperatures T_p and T_s equal to the air temperature T_a, calculate the conductances h_c, h_r and h_m, then solve eq 35 and 36 for new temperatures using these to calculate new conductances and continue the process until the temperatures converge. The convergence is found to improve considerably by averaging the temperatures obtained in each iteration.

There is a small loss of energy by conduction from the snow and heating panel surfaces through the duct wall. This is accounted for by adding the thermal conductance by conduction to the convection conductances h'_c and h_c.

As explained earlier, eq 32 is likely to predict lower heat transfer rates to the snow surface since it does not take into account the variation in configuration factor and the nonisothermal character of the radiation to the snow surface. To take these effects into account, the duct is divided into 12 zones along its length (6 in. long, 20 in. wide). The temperature of each zone is assumed uniform. The initial values for the zone temperatures are found by the above thermal network which is applied at successive distances x from the entrance. The radiation to each zone on the snow surface R_i is then given by eq 12 and the radiation from each zone on the heating panel P_i is given by eq 13. An energy balance at the heating panel surface gives:

$$T_p = \frac{Q - P_i + h'_c \, T_a}{h'_c} \, . \tag{36}$$

Similarly an energy balance at the snow surface yields:

$$T_s = \frac{R_i + h_c \, T_a + h_m \, T_{dp}}{h_c + h_m} \, . \tag{36a}$$

Equation 36a must itself be solved by iteration since h_m is a function of the snow temperature T_s. The values of T_p and T_s calculated from eq 36 and 36a can then be used in eq 12 and 13 to calculate new values for the radiation heat transfer to and from the zones on the snow and heating panel surfaces. Again the convergence is improved considerably by averaging the temperatures obtained in each iteration.

Equations 32, 33, 34, 35, and 36 serve to relate the independent variables T_a, T_{dp}, V, and Q to the dependent variables T_p and T_s and ultimately to the mass transfer $\frac{g}{A}$. In general, the independent variables are uncertain. In view of the fact that there are four independent variables, the variance of the sublimation rate will necessarily be greater than the variance of any one of the independent variables. Further, the effect of a small variation in one of the independent variables is likely to produce a larger variation in a mass transfer rate. The net effect is that the mass transfer rate is quite likely to be more uncertain than all of the independent variables.

Tribus and Roe [1964] present a method for handling this problem. They have shown that the variance of a system response is related to the variance of the parameters by the following:

$$\sigma^2 (f) = \sum_i \left[\frac{\delta f}{\delta x_i} \right]^2_{x_i = \overline{x_i}} \sigma^2 (x_i) \tag{37}$$

where the system response is f and the x's represent the parameters. This equation is valid provided that the deviation around the expected value of the parameters is approximately symmetrical, and that second order derivatives of the response with respect to the parameters are negligible. For the purpose of this analysis, we will assume the simplifications are valid.

Letting the response function be represented by the mass transfer rate, and the parameters by the independent variables, we may write:

$$\sigma^2\left(\frac{g}{A}\right) = \left[\frac{\delta\left(\frac{g}{A}\right)}{\delta V}\right]^2_{v=\overline{v}} \sigma^2(V) + \left[\frac{\delta\left(\frac{g}{A}\right)}{\delta T_a}\right]^2_{T_a=\overline{T}_a} \sigma^2(T_a) + \left[\frac{\delta\left(\frac{g}{A}\right)}{\delta T_{dp}}\right]^2_{T_{dp}=\overline{T}_{dp}} \sigma^2(T_{dp}) + \left[\frac{\delta\left(\frac{g}{A}\right)}{\delta Q}\right]^2_{Q=\overline{Q}} \sigma^2(Q) \quad (38)$$

A digital computer was used to solve the thermal network by the iteration method presented above. The variables T_a, T_{dp}, V and Q were varied systematically to determine the variation in mass transfer rate due to small fluctuations in the variables. The derivatives in eq 38 were estimated graphically and the variance of the mass transfer rate calculated. The computer program and the results obtained from the program are presented in Appendix H.

The results for two different sets of values for the independent variables T_a, T_{dp}, V, Q are presented in Figures 2, 3, and 4. The dashed line corresponds to the approximate solution for snow temperature and mass transfer obtained by assuming the radiation to be isothermal (eq 32). The solid line represents the solution obtained by the second method described above which accounts for the nonisothermal radiation. The error bars on the solid line in Figures 3 and 4 represent the standard deviation ($\sigma(g/A)$) calculated from eq 38. The standard deviation for the high temperature run (T_a = 21.5F, Fig. 4) is larger because the uncertainty in the dewpoint temperature affects the mass transfer rate to a greater degree.

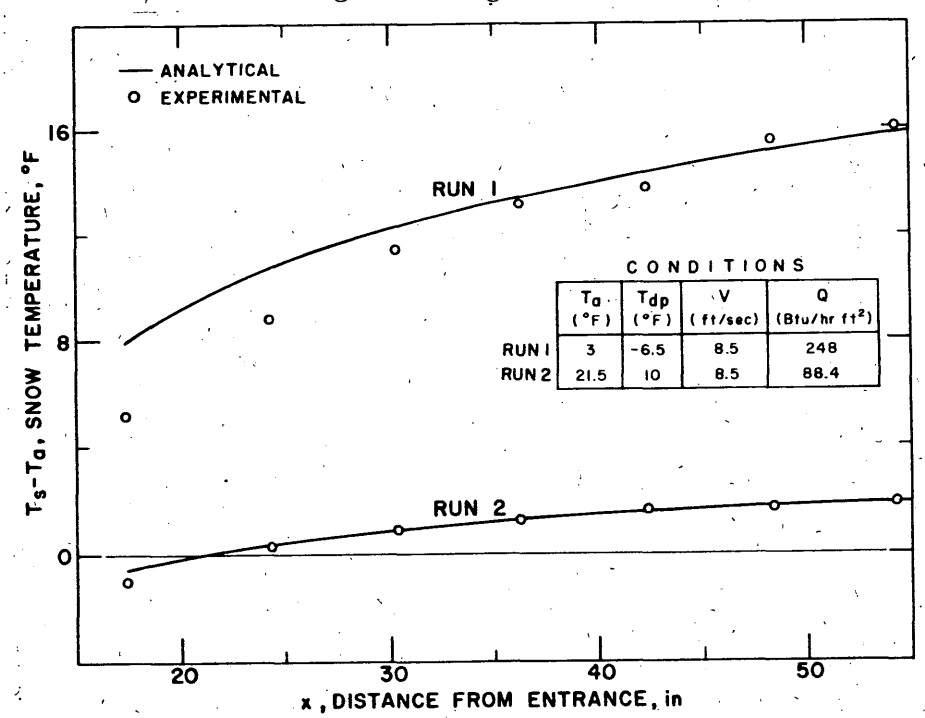

Figure 2. Snow temperature difference vs distance from entrance.

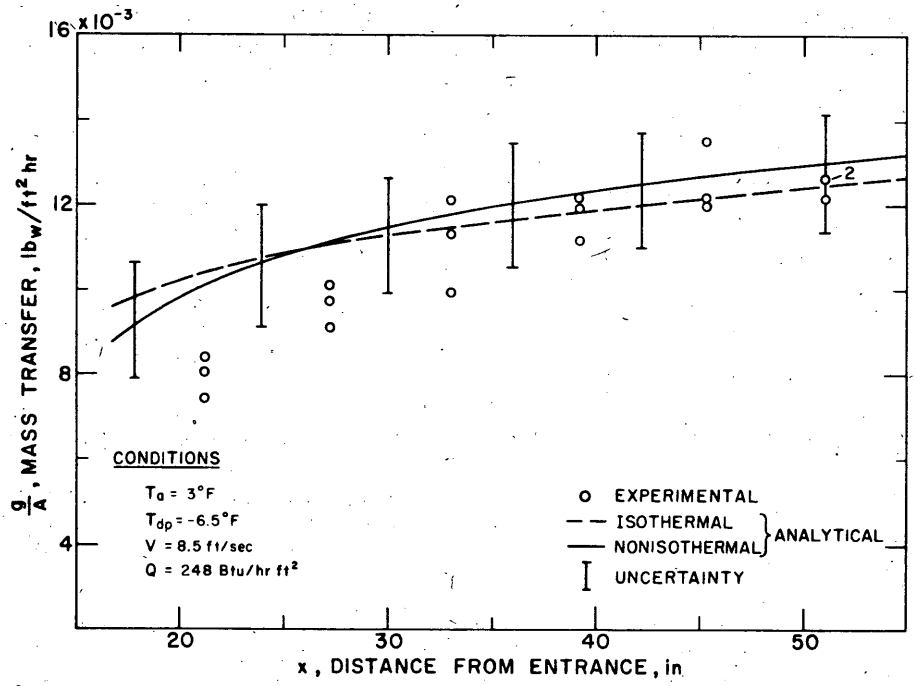

Figure 3. Mass transfer vs distance from entrance, Run 1.

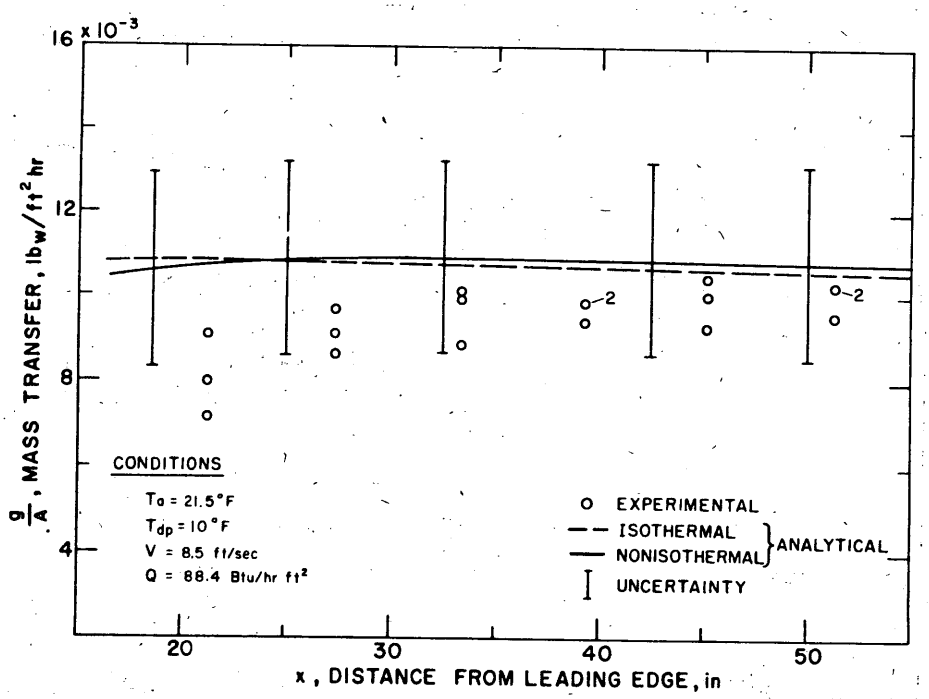

Figure 4. Mass transfer vs distance from entrance, Run 2.

V. EXPERIMENTAL PROCEDURE

The experimental apparatus consisted of a rectangular duct constructed of plywood and Plexiglas having a height of 5 in., width 20 in., and length 96 in. (Fig. 5). A strip of Teledeltos electrical resistance paper was stretched over the roof of the duct to provide a uniform heat source. The floor of the duct was covered with a thin layer of snow. Air was drawn through the duct by a fan at a velocity of 8.5 ft/sec. The entire apparatus was placed in a cold room and the temperature was kept below 32F to prevent melting of the snow.

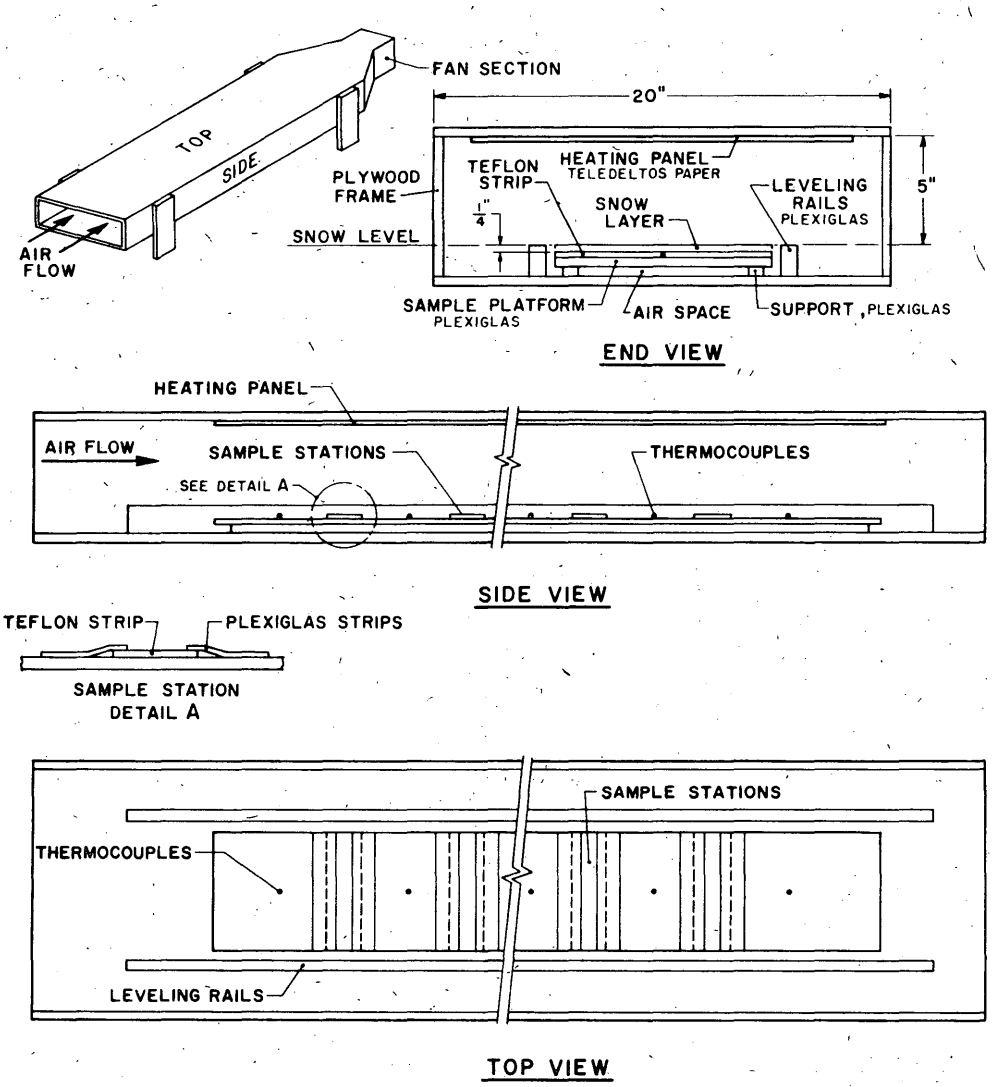

Figure 5. Diagram of the experimental apparatus.

Thermocouples were located 1/4 in. below the snow surface to measure the surface temperature. The resistance to heat transfer, by conduction through the wall of the duct, from the thermocouples to the air ($\simeq$ 7.2F-hr-ft^2/Btu) is quite large compared to the resistance from the snow surface to the thermocouples ($\simeq$.02F-hr-ft^2/Btu). Hence the thermocouples may be considered to measure the snow surface. This was checked experimentally by watching for a temperature increase as the snow surface sublimed toward the buried thermocouples; there was no indication of an increase.

The sampling stations shown in Figure 5 were Teflon strips held down by Plexiglas strips. They were 6 in. long placed 3 in. on each side of the center of the duct. Samples of the snow at these stations were taken periodically and the time between samplings was recorded. The sampling tool used was a thin-walled aluminum tube (0.434 in. diam). The tube was forced through the snow at the sampling stations until it touched the Teflon strips. The snow in the tube was compressed with a rod to increase its adhesion to the inside walls of the tube. The sample was then extracted, sealed in a weighing bottle, and weighed on an analytical balance. The difference in weight of two samples taken at the same station was divided by the cross-sectional area of the tube and the elapsed time between samplings to obtain the sublimation rate.

The free stream velocity in the duct was measured by a Pitot tube connected to a micromanometer, and this measurement was checked by a hot wire anemometer. The velocity was found to be unsteady. The fluctuations were approximately 5% of the mean velocity in the free stream.

The wet bulb temperature in the cold room was measured by an Assmann psychrometer. The free stream air temperature and dewpoint in the duct were assumed to be the same as the temperature and dewpoint in the room.

The heating panel was energized by a Variac coupled to a transformer. The energy dissipated in the resistance paper was found by taking the product of the RMS voltage drop across the paper and the current drawn by the paper.

The experimental procedure was to set the room temperature, the voltage across the heating panel, and the air velocity. Time was then allowed for the system to come to steady state temperature. This was usually about 2 to 3 hours. The snow was smoothed by running a metal bar over the Plexiglas rails. Initial weights of the snow at the six weighing stations were then taken.

The experiment was run for about 1 to 2 days to allow a significant mass transfer from the surface to take place. The snow surface temperature was measured continuously during these runs with a 16-channel millivolt recorder. The snow temperature was found to fluctuate no more than 0.1 to 0.2F during the runs, while the air temperature fluctuated about 1 to 2F. The air temperature and snow temperature were raised about 4 to 8F during the defrost cycle of the room, but the effect of the defrost cycle was considered to be negligible since the system underwent a significant temperature rise only 3% of the total time. The dewpoint and velocity were checked periodically throughout the run.

After the system had been run for 1 to 2 days, the elapsed time for the run was recorded and the final snow samples were taken. The initial samples were taken at the edges of the sampling stations (3 in. off the center line of the duct, Fig. 5) and the final samples were taken at the center line. This was done to avoid the "wake" caused by holes left in the snow after the initial samples were taken, which would have affected the final samples taken at downstream stations. Actually this effect was quite pronounced and it was

possible to see a trough left behind the original samples for about 6 in. downstream. The holes apparently induced a vortex in the boundary layer approximately the width of the hole (~.45 in.), producing a greater mass transfer rate in the wake.

The accuracy of the mass transfer measurements depends on the ability to make a uniform snow thickness and density at a given sampling station. It was found that, when the snow was carefully sifted into a sampling station, samples taken over the station would have the same weight to within 7%. Since the mass transfer measurements were based on the difference between the initial and final weights after approximately 2/3 of the snow at the stations had been sublimed, the error in the mass transfer measurements was expected to be about 10%. This is apparent in the spread of the data indicated in Figures 3 and 4.

VI. RESULTS AND DISCUSSION

The analytical and experimental results shown in Figures 2, 3, and 4 indicate that mass transfer rates can be predicted in the duct model with uncertainties of from 13 to 20%. The present experiment does not allow the determination of mass transfer rates to any greater degree of accuracy since the uncertainties have their origin in the inability to control as well as measure the independent variables T_a, T_{dp}, V, and Q. The analysis, however, is adequate for the prediction of mass transfer rates in snow tunnels. A suitable safety factor may be incorporated in the design of a snow removal system to allow for the uncertainties in the mass transfer rate.

The contribution of this investigation has been threefold. First, the relative importance of the various factors which affect the mass transfer rate has been determined. Secondly, an analysis has been developed to predict the mass transfer rate when the independent parameters T_a, T_{dp}, V, and Q are known. Thirdly, the analysis has been verified by experimental data to within the accuracy of the independent variables in the experiment.

It has been shown that a non-uniform surface temperature of up to 20F on the heating panel has a negligible effect on the mass transfer rate. The non-isothermal snow surface does not significantly alter the mass transfer coefficient and the mass transfer rate. The accelerated flow in the entrance region does not significantly affect the mass transfer rate and hence the forced convection heat and mass transfer can be considered to be of the "flat plate" type (zero pressure gradient, and zero acceleration in the free stream).

The roughness of the snow surface in the present investigation (k_s ~0.02 in.) is less than that which might be encountered in practice. But the influence of roughness on the mass transfer is determined by the parameter k_s/x, where x is the distance from the entrance; hence surface protrusions of up to 0.2 in. may be allowed in the snow tunnels without any significant effect on the mass transfer rate.

The factors which are seen to influence the mass transfer are, in their order of importance: the air velocity V, the air temperature T_a, the air dewpoint temperature T_{dp}, and the strength of the power source Q. This order is changed somewhat for extreme conditions. For instance, at higher air temperatures (T_a ~20F), the mass transfer rate is not affected so much by velocity as it is by dewpoint temperature. In general, the calculations become sensitive to the dewpoint temperature when the snow surface temperature is held only a

little above the air temperature. This, of course, is necessary at the higher air temperatures to avoid excessive deformation or melting of the snow.

Several important conclusions may be reached with regard to the design of undersnow camps where the attempt is made to control closure by mass transfer from the walls. It is assumed that a uniform, predictable mass transfer rate from every snow wall in the network of tunnels is desired.

First, changes in cross-sectional area in the free space of snow tunnels should be minimized. Clearly the design of Camp Century (Fig. 1) is inadequate in this respect. There are large spaces between the buildings where the air velocity, and hence the mass transfer rate, would be significantly retarded. There is an abrupt change in cross-sectional area at the entrance to the tunnel, making the flow velocity highly non-uniform. Thus large variations would appear in the mass transfer rate near the entrance.

Secondly, the air temperature and dewpoint must be carefully controlled since mass transfer rates are highly dependent on these factors. Extraneous sources of energy such as heat given off by buildings, combustion engines, etc., would have to be minimized by adequate insulation. Sources of water vapor would have to be eliminated or minimized. The ventilation of the entire tunnel network would have to be regulated as regards temperature and humidity. The design air temperature will have to be decided on the basis of other considerations as well as the desired mass transfer rate (e.g., the temperature must not be so high as to cause excessively high deformation of the snow wall) but, assuming the design temperature to be approximately 10F, the ventilation system must be capable of heating as well as cooling the air.

On the basis of this investigation and the work of Lamb [1964], the best method for introducing power into the snow surface seems to be irradiation of the snow surface. This conclusion is based on the assumption that the objective is to achieve a uniform, predictable sublimation rate in the tunnel. While Lamb showed that the efficiency of the method of direct energy input into the snow surface (by heated wires) was greater than for irradiation of the snow surface, it is clear from this investigation that the air temperature and dewpoint temperature must be accurately controlled and the cost of such an extensive ventilation system would far outweigh the cost of a loss in efficiency by using the radiation method. The importance of having a uniform, predictable mass transfer rate will have to be weighed against its excessive cost in the initial stages of the design of future undersnow camps.

The analysis presented here is felt to be generally applicable for predicting mass transfer rates from snow surfaces. Excessive conduction through the snow surface may be taken into account by simply including another conductance in the thermal network analysis. Changes in the mass transfer rate due to alterations in the flow (e.g., excessive pressure gradients, laminar flow instead of turbulent flow, etc.) may be accounted for by altering the convection conductances in the network. High temperature radiation into the snow surface may be handled by a suitable alteration [Poppendiek and Tribus (1961)]. In general the network analysis method for predicting the combined energy transfer by radiation, forced convection, and sublimation mass transfer from a snow surface is seen to be flexible and adequate for the prediction of mass transfer rates.

The experimental data are able to verify the analysis only to within uncertainties of 10 to 20%. However, since the uncertainties in temperature and dewpoint encountered in practice will necessarily be greater than in the controlled experiment and safety factors of at least this order must be introduced in the design of a mass transfer system, the experimental verification is felt to be adequate.

LITERATURE CITED

Blasius, H. (1932) Das Ähnlichkeitsgesetz bei Reibungsvorgangen in Flussigkeiten, Forsch. Ing. - Wes., no. 356.

Chilton, T.H. and Colburn, A.P. (1934) Industrial and engineering chemistry, vol. 26, no. 11.

Dorsey, N.E. (1940) Properties of ordinary water-substance. New York: Reinhold Publishing Company.

Hamilton, D.C. and Morgan, W.R. (1952) Radiant interchange configuration factors, NACA Technical Note 2836.

Lamb, W.D. (1964) Investigations of thermal means of snow removal in under-snow camps, CRREL Project DA-AMC-27-021-63-GI, Report No. 3, Thayer School of Engineering, Dartmouth College, Hanover, N.H. (unpublished).

Nikuradse, J. (1933) Stromungsgesetze in rauhen Rohren, Forsch. Gebiete Ingenieurw, no. 361.

Oppenheim, A.K. (1956) Radiation analysis by the network method, American Society of Mechanical Engineers Transactions, vol. 78, p. 725.

Poppendiek, H.F. and Tribus, M. (1951) A comparison of several heat and mass transfer networks of interest in water conservation, Transactions American Geophysical Union, vol. 32, no. 1.

Reynolds, W.C., Kays, W.M., and Kline, S.J. (1957) Heat transfer in the turbulent incompressible boundary layer with a step wall temperature distribution, Final Report, Part II, Contract NAw-6494, NACA, Department of Mechanical Engineering, Stanford University, Stanford, California.

Rohsenow, W.M. and Choi, H. (1961) Heat, mass, and momentum transfer. Englewood Cliffs, N.J.: Prentice Hall, Inc.

Rubesin, M.W. (1951) The effect of an arbitrary surface temperature variation along a flat plate on the convective heat transfer in an incompressible turbulent boundary layer, NACA Technical Note 2345.

Schlichting, H. (1960) Boundary layer theory. New York: McGraw-Hill Book Company.

Shapiro, A.H. (1954) The dynamics and thermodynamics of compressible fluid flow, Vol. II, Ronald Press Company.

Tribus, M. and Klein, J. (1953) "Forced convection from nonisothermal surfaces," Chapter 8 in Heat transfer-A symposium. Ann Arbor, Michigan: University of Michigan Press.

Tribus, M. and Roe, P.H. (1964) Prediction of the response of linear systems with uncertain parameters, International Conference on Microwaves, Circuit Theory, and Information Theory, Tokyo, Japan, September, 1964.

von Karman, Th. (1921) On laminar and turbulent friction, Zeitschrift für angewandte Mathematik and Mechanik, vol. 1, no. 4. NACA Technical Memorandum 1092, 1946.

APPENDIX A. DETERMINATION OF THE EMISSIVITY OF THE RESISTANCE PAPER

A radiometer was used to measure the emissivity of the Teledeltos resistance paper used in the experiment. The radiometer consisted of an aluminum cone with a shielded and an active thermistor at the vertex of the cone. The active thermistor was raised in temperature a small amount by the radiant energy impinging on it from a laboratory blackbody (a Leslie cube). The circuitry of the radiometer measured the temperature difference between the two thermistors and displayed a meter deflection which was linear in the temperature difference. For small temperature differences, the incoming radiant energy was assumed proportional to the temperature differential.

One side of the Leslie cube was a blackened small angle wedge which was considered to be a blackbody. The Teledeltos paper was stretched tightly on one of the other sides. The cube was filled with water to regulate the temperature.

The procedure of the experiment was to take two cubes filled with water at different temperatures. The meter deflections of the radiometer were observed for Teledeltos paper and the blackbody for the two cubes. The measurements were taken quickly to minimize the possibility of the temperature of either the shielded thermistor or the cubes changing during the experiment. The differences in the meter deflections ΔMD for the two cubes were recorded and the emissivity calculated from the following relationships:

Blackbody:

$$\Delta MD \propto \Delta\left(\frac{q}{A}\right)_{net} = \sigma(T_H^4 - T_c^4)$$

Teledeltos:

$$\Delta MD \propto \Delta\left(\frac{q}{A}\right)_{net} = \sigma \epsilon (T_H^4 - T_c^4)$$

$$\frac{\Delta MD_{TEL}}{\Delta MD_{BB}} = \epsilon .$$

These relationships hold provided the temperature of the shielded thermistor and the temperatures of the cubes do not change during the measurements. It was possible to check these assumptions by noting the meter deflection of a constant temperature body before and after the experiment and measuring the temperature of the cubes before and after the experiment. It was found that the temperatures did not change significantly.

It is necessary also to estimate the temperature drop across the Teledeltos paper to insure that it was the same temperature as the blackbody. Assuming that the thermal conductivity of paper is $.075 \frac{\text{Btu/hr-ft}}{\text{F}}$ and allowing for 1/2 paper thickness (= .004 in.) air space between the cube and the paper, the resistance to energy transfer is $.017 \frac{\text{hr-ft}^2\text{-F}}{\text{Btu}}$. The energy transfer coefficient for free convection is approximately $1.0 \frac{\text{Btu}}{\text{hr-ft}^2\text{-F}}$ so the temperature drop across the paper is only 1.7% of the total and hence may be neglected. The emissivity of the Teledeltos paper was measured to be $0.75 \pm .05$.

APPENDIX B. NONISOTHERMAL RADIATION CONFIGURATION FACTORS

In order to estimate the effect of nonisothermal radiation on the snow surface, the duct is divided into isothermal sections as shown below:

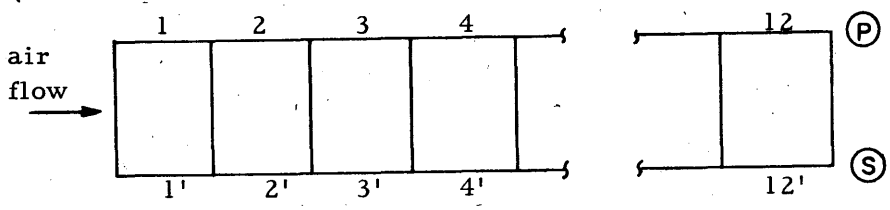

The sections 1 to 12 represent 1/2-ft divisions along the length of the heating panel (see diagram of experimental apparatus, Fig. 5). Since the experimental points were taken from about 20 to 60 in. downstream from the duct opening, we are interested particularly in this region.

In order to solve this problem, it is necessary to compute the fraction of radiation emitted by a section on the panel which is intercepted by a section on the snow surface. We can see by inspection of the diagram above that it is only necessary to calculate 12 configuration factors, $F_{11'}$, $F_{12'}$, $F_{13'}$, ... $F_{1\,12'}$, since all others are determined from these by symmetry. The configuration factor $F_{11'}$ can be computed from eq 4. With x = 6/5, y = 20/5 eq 4 yields: $F_{11'} = 0.39$. The other configuration factors may be computed by the use of configuration factor algebra; the rules of configuration factor algebra are given below.

$$2\,F_{12}{}^{2} = F_{1(1'2')} + F_{2(1'2')}$$

$$= F_{11'} + F_{12'} + F_{21'} + F_{22'}$$

where $F_{12}{}^{2} = F_{(12)\,(1'2')}$ or the fraction of radiation emitted by the zones 1 and 2 which is intercepted by the zones 1' and 2'. These rules apply only to zones with equal areas. The rules for zones of unequal areas are given in Hamilton and Morgan, 1952. Using the above rule, and the symmetry of the diagram above, the configuration factors are:

$$F_{12'} = F_{12}{}^{2} - F_{11'}$$

$$F_{13'} = 3/2F_{123}{}^{2} - F_{12}{}^{2} - F_{12'} - \frac{F_{11'}}{2}$$

$$F_{14'} = 2F_{1234}{}^{2} - 3/2F_{123}{}^{2} - F_{13'} - F_{12'} - \frac{F_{11'}}{2}$$

$$F_{15'} = 5/2F_{12345}{}^{2} - 2F_{1234}{}^{2} - F_{14'} - F_{13'} - F_{12'} - \frac{F_{11'}}{2}$$

$$F_{16'} = 3F_{123456}{}^{2} - 5/2F_{12345}{}^{2} - F_{15'} - F_{14'} - F_{13'} - F_{12'} - \frac{F_{11'}}{2}$$

The configuration factors of order higher than $F_{16'}$ will be neglected (i.e., the radiation from zones more than 3 ft upstream or downstream in the duct

will be neglected). The configuration factors $F_{12}{}^2$, $F_{123}{}^2$, etc. may be calculated from eq 4; they are:

$$2F_{12}{}^2 = 2F(12/5, 4) = 1.093$$
$$3F_{123}{}^2 = 3F(18/5, 4) = 1.851$$
$$4F_{1234}{}^2 = 4F(24/5, 4) = 2.622$$
$$5F_{12345}{}^2 = 5F(30/5, 4) = 3.398$$
$$6F_{123456}{}^2 = 6F(36/5, 4) = 4.176$$

These values are then used to obtain the final configuration factors:

$$F_{11'} = 0.39$$
$$F_{12'} = 0.1566$$
$$F_{13'} = 0.2714 \times 10^{-1}$$
$$F_{14'} = 0.6847 \times 10^{-2}$$
$$F_{15'} = 0.2410 \times 10^{-2}$$
$$F_{16'} = 0.1045 \times 10^{-2}$$

Since the configuration factors are now known, it is possible to solve the network for the problem which is shown in part in section I. Consider the i^{th} node of the radiation network shown below.

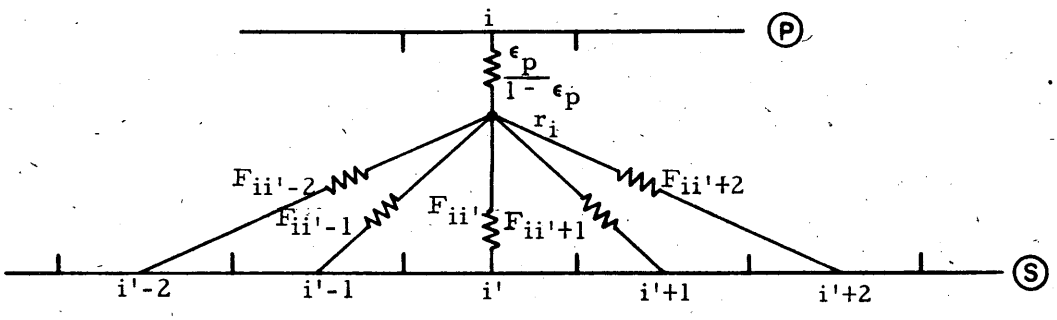

The paths i to i' + 3, etc. are not shown above and the paths i to i' + 6 and above were found to transfer a negligible amount of energy. The above network is equivalent to the network shown below.

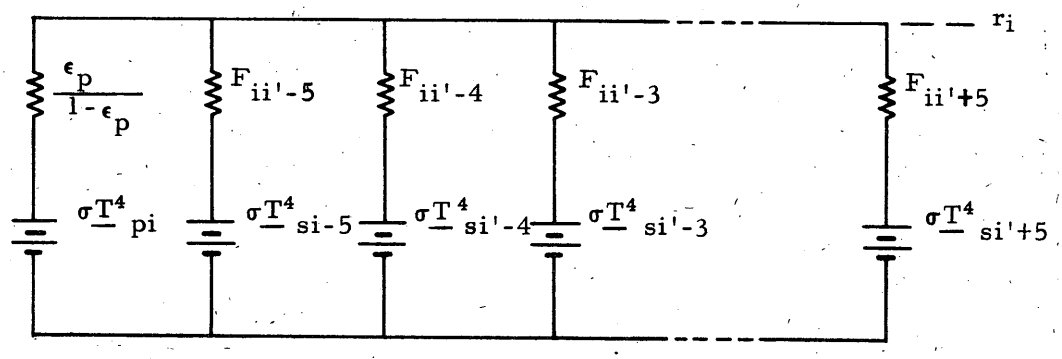

APPENDIX B

This network may be simplified to:

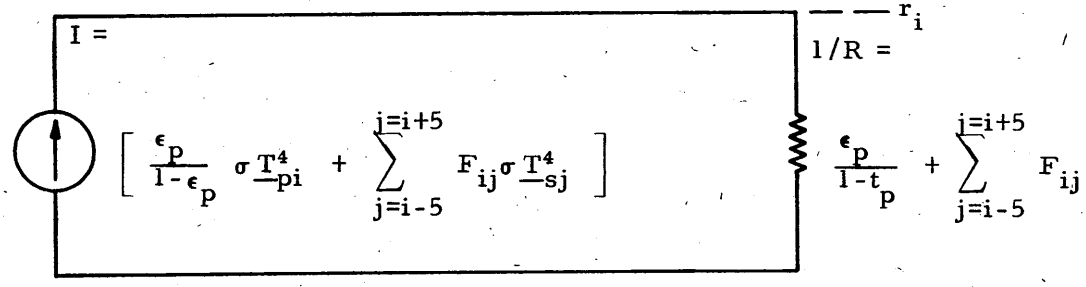

The node potential r_i is given by the product of the current I and the resistance R which is:

$$r_i = \frac{1}{\frac{\epsilon_p}{1-\epsilon_p} + \sum_{j=i-5}^{j=i+5} F_{ij}} \left[\frac{\epsilon_p}{1-\epsilon_p} \sigma \underline{T}_{pi}^4 + \sum_{j=i-5}^{j=i+5} F_{ij} \sigma \underline{T}_{sj}^4 \right]$$

This will be recognized as eq 11.

APPENDIX C. DERIVATION OF THE INTEGRAL EQUATIONS FOR THE BOUNDARY LAYER

Consider the heat, mass and momentum transport across the boundary layer over a flat plate shown below:

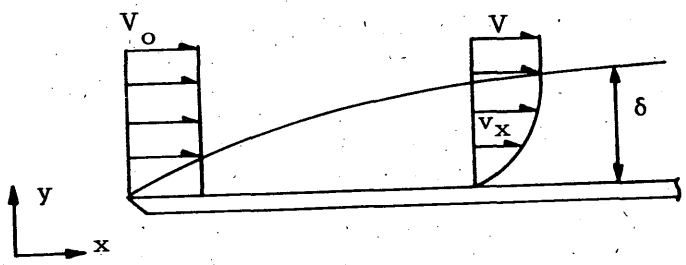

Assume that the air flow over the plate is steady, two-dimensional, and incompressible; also that the flow in the boundary layer is turbulent from the leading edge of the plate (x=0, y=0). The surface of the plate is heated and saturated with water vapor so that heat and mass transfer occurs from the plate to the free stream air. The surface temperature of the plate is assumed to be constant. The free stream air temperature and dewpoint temperature are assumed constant, but the free stream air velocity is increasing in the x direction. The boundary layer thickness δ indicated above is defined as the distance from the plate where the velocity has been retarded by 1% of the free stream.

$$v_x = 0.99V \text{ at } y = \delta \qquad \text{(C1)}$$

The boundary layer thickness increases in the x direction because the air particles near the plate are continually being retarded as they proceed downstream. This process may be visualized as a transport of momentum from the free stream to the flat plate.

Heat transfer and mass transfer occur from the plate to the free stream in a manner analogous to the transfer of momentum from the free stream to the plate. A thermal gradient is established at the surface of the plate and extends farther out from the plate at increasing distances from the edge of the plate. A humidity (moisture content of the air) gradient is established in an analogous manner. Thermal and humidity boundary layer thicknesses may be defined in the same manner as was the velocity boundary layer thickness.

$$\theta = \frac{T-T_s}{T_a-T_s} = 0.99 \text{ at } y = \delta'$$

$$\phi = \frac{H-H_s}{H_a-H_s} = 0.99 \text{ at } y = \delta'' \qquad \text{(C2)}$$

where T_a, T_s, H_a, and H_s are the air temperature, snow surface temperature, air humidity ratio (mass of water vapor per unit mass of air), and snow surface humidity ratio respectively.

Figure C1 describes the flow in the boundary layer in a particularly convenient way. A differential control volume is drawn over the height of the boundary layer. The mass flow of air crossing the boundaries of the control volume is shown in Figure C1a; the forces on the control surface and the momentum crossing the boundaries of the control volume are shown in Figure C1b. Figure C1c and d show the energy crossing the control surface and the water vapor flux at the control surface, respectively. The quantities i_a and H_a denote the enthalpy and humidity ratio of the air respectively. The momentum equation requires that the net force on the control surface in the x direction balance the net efflux of momentum from the control volume. The energy and mass conservation laws require that the net heat and mass transfer into the control volume balance the net efflux of enthalpy, and mass from the control volume respectively. These three requirements may be written:

Momentum:

$$-\delta \frac{dp}{dx} - \tau_w = \frac{d}{dx} \int_0^{\delta} \rho v_x^2 \, dy - V \frac{d}{dx} \int_0^{\delta} \rho v_x \, dy \qquad (C3)$$

Energy:

$$q = \frac{d}{dx} \int_0^{\delta'} \rho v_x i \, dy - i_a \frac{d}{dx} \int_0^{\delta'} \rho v_x \, dy \qquad (C4)$$

Mass:

$$g = \frac{d}{dx} \int_0^{\delta''} \rho v_x H \, dy - H_a \frac{d}{dx} \int_0^{\delta''} \rho v_x \, dy \, . \qquad (C5)$$

If the specific heat of the air is constant over the temperature range considered, the enthalpy may be replaced by:

$$i - i_a = c_p (T - T_a) \, . \qquad (C6)$$

The flow in the free stream is not affected by shearing stresses and hence may be considered to be ideal or potential flow. The pressure gradient may then be expressed in terms of the free stream velocity with Euler's equation:

$$\frac{dp}{dx} = -\rho V \frac{dV}{dx} \, . \qquad (C7)$$

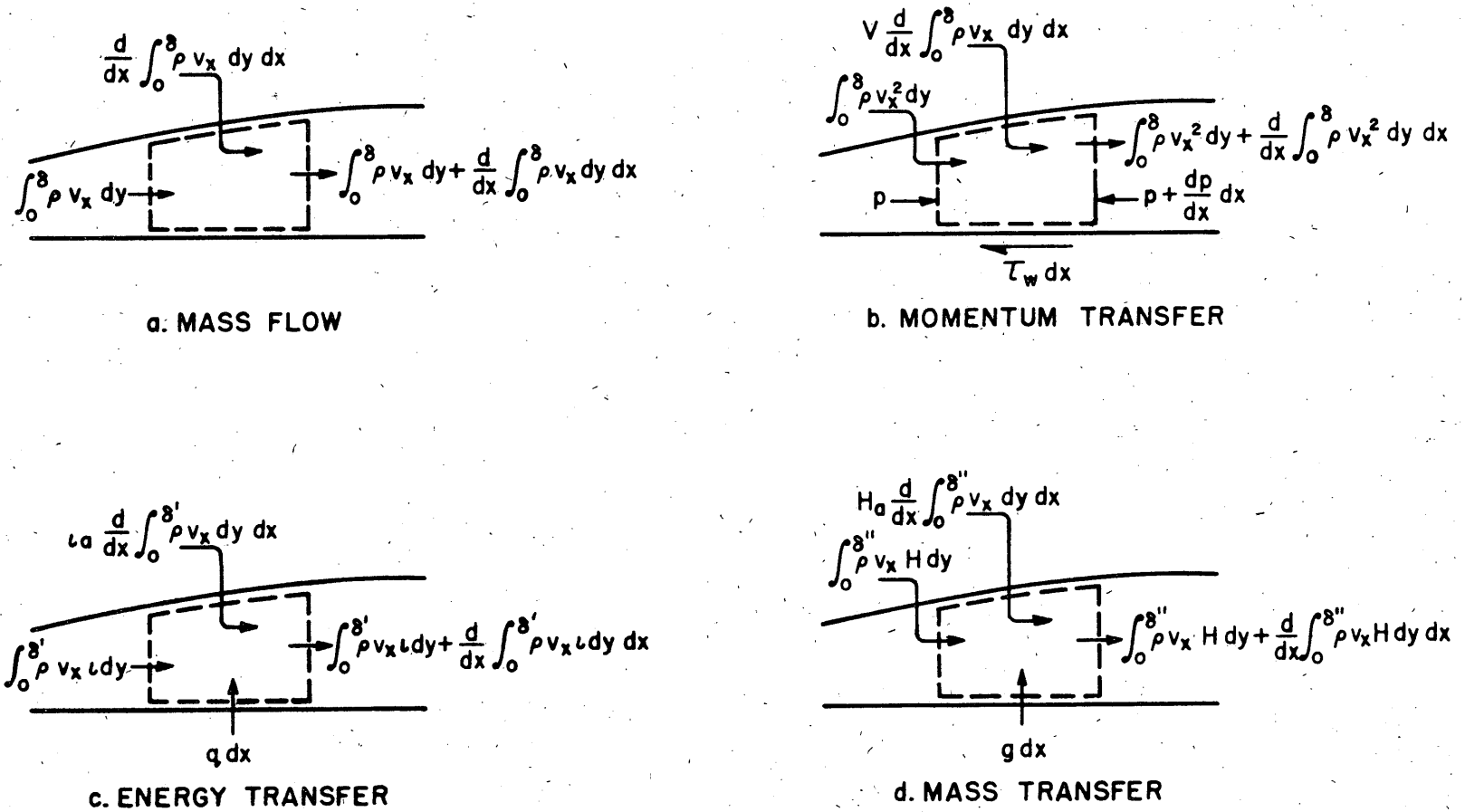

Figure C1. Steady, two-dimensional, incompressible, turbulent flow in a boundary layer over a flat surface.

APPENDIX C

Assume that the fluid properties (c_p, ν) are constant. Inserting eq C6 and C7 into eq C4 and C3 respectively, and making use of the above assumptions, there is obtained after some rearrangement,

Momentum:

$$\frac{\tau_w}{\rho V^2} = \frac{1}{V}\frac{d}{dx}\int_0^{\delta} v_x\,dy - \frac{1}{V^2}\frac{d}{dx}\int_0^{\delta} v_x^2\,dy + \frac{\delta}{V}\frac{dV}{dx} \qquad \text{(C8)}$$

Energy:

$$St = \frac{q}{\rho c_p V(T_s - T_a)} = \frac{1}{V}\frac{d}{dx}\int_0^{\delta'} v_x\,dy - \frac{1}{V}\frac{1}{dx}\int_0^{\delta'} \theta v_x\,dy \qquad \text{(C9)}$$

Mass:

$$\frac{h_D}{V} = \frac{g}{\rho V(H_s - H_a)} = \frac{1}{V}\frac{d}{dx}\int_0^{\delta''} v_x\,dy - \frac{1}{V}\frac{d}{dx}\int_0^{\delta''} \phi v_x\,dy\,. \qquad \text{(C10)}$$

APPENDIX D. DERIVATION OF FORMULAS FOR SHEAR STRESS AND BOUNDARY LAYER THICKNESS:

ADAPTATION OF PIPE DATA TO FLOW OVER A FLAT PLATE

Schlichting [1960] presents an excellent review of the results of numerous investigators concerning the relation between skin friction and Reynolds number for fully developed turbulent flow through pipes. In general, the skin friction C_f is dependent on the pipe Reynolds number $\rho\frac{\overline{V}d}{\mu}$, and the surface roughness parameter $\frac{k_s}{d}$, where k_s is the dimension of the mean surface protrusion and d is the pipe diameter. For smooth pipes ($\frac{k_s}{d} << 1$), the data can be correlated by the well known Blasius formula:

$$\frac{C_f}{2} = (0.0396)\left(\rho\frac{\overline{V}d}{\mu}\right)^{-1/4} \tag{D1}$$

for pipe Reynolds numbers less than 10^5. This relation must be replaced by a logarithmic law for higher Reynolds numbers. Surface roughness tends to increase the skin friction and reduce the dependence on Reynolds number. For a "completely rough" pipe, the skin friction is dependent only on the relative roughness and not on the Reynolds number.

Prandtl first showed that the Blasius skin friction law requires that the velocity distribution in the pipe follow a 1/7 power law:

$$\left(\frac{v_x}{V_{max}}\right) = \left(\frac{y}{r}\right)^{1/7} . \tag{D2}$$

This distribution agrees with experiments quite well up to Reynolds numbers of 10^5, which is the limit for the Blasius formula [Schlichting, 1960].

von Karman first used the following method for adapting these results to flow over a flat plate. The adaptation can be made because of the similarity exhibited by velocity profiles in pipes of different diameters. Relation D2 retains its validity regardless of the pipe diameter. His method is presented in outline form here; the reader may also consult von Karman (1921).

For steady, two-dimensional, incompressible flow over a smooth flat plate (Fig. C1), a momentum valance yields:

$$\frac{-\tau_w}{\rho} = \frac{d}{dx}\int_0^{\delta} v_x^2\, dy - V\frac{d}{dx}\int_0^{\delta} v_x\, dy . \tag{D3}$$

Because of the similarity exhibited by eq D2 for pipes of different diameters, we expect relation D2 to hold for a flat plate, with the boundary layer thickness replacing the tube radius and the free stream velocity replacing the maximum or center line velocity in the pipe:

$$\frac{v_x}{V} = \left(\frac{y}{\delta}\right)^{1/7} \tag{D4}$$

provided the Reynolds number based on the boundary layer thickness ($\rho \frac{V\delta}{\mu}$) does not exceed 10^5. The formula for skin friction may be adapted in the same manner:

$$\frac{C_f}{2} = 0.0233 \left(\rho \frac{V\delta}{\mu}\right)^{-1/4} \quad \text{(D5)}$$

These relations are inserted into eq D3 to obtain a differential equation for the boundary layer thickness:

$$\frac{7}{72} \frac{d\delta}{dx} = 0.0233 \left(\frac{V\delta}{\nu}\right)^{-1/4} \quad \text{(D6)}$$

This equation may be readily integrated to obtain:

$$\delta(x) = 0.382\, x \left(\frac{Vx}{\nu}\right)^{-1/5} \quad \text{(D7)}$$

Inserting this relation into eq D5 results in:

$$\frac{C_f}{2} = 0.0296 \left(\frac{Vx}{\nu}\right)^{-1/5} \quad \text{(D8)}$$

This is valid for length Reynolds numbers ($\frac{Vx}{\nu}$ not exceeding 10^6.

When von Karman originally derived eq D5, he assumed a different numerical value for the ratio of mean pipe velocity to maximum pipe velocity ($\frac{\overline{V}}{V_{max}} = 0.84$) than that dictated by the 1/7 velocity distribution ($\frac{\overline{V}}{V_{max}} = 0.816$). This was based on the somewhat limited experimental data available at the time and the effects of pipe roughness were not well understood. The experiments of Nikuradse [1933], however, have indicated that the 1/7 velocity distribution is valid for moderate Reynolds numbers in smooth pipes and thus the value of $\frac{\overline{V}}{V_{max}}$ equal to 0.816 should be used in the adaptation. When this value is used to derive eq D5, the numerical factor 0.0233 is obtained. von Karman obtained the value 0.0225.

Since the 1/7 distribution is used in obtaining eq D6, there seems to be theoretical as well as experimental justification for favoring the numerical constant 0.0233 over 0.0225. When the value 0.0233 is used to derive eq D8, the results show 3% better agreement with the available experimental data for flow over a flat plate (Rohsenow and Choi, 1961; Schlichting, 1960). This point has not been recognized in the literature (ibid) and eq D8 is obtained by arbitrarily adjusting the incorrect numerical factor obtained by von Karman to 0.0233 to agree with experiment. The preceding argument has shown that when the pipe formulas are correctly adapted for flat plate flow, excellent agreement with experiment is obtained without any necessity to adjust the numerical factors.

APPENDIX E. ENTRANCE EFFECTS

It was shown in Appendix D that for Reynolds numbers less than 10^5 similar velocity profiles are exhibited by fully developed flow in smooth pipes of different diameters. It was for this reason that the equation for pipe flow could be readily adapted to flow over a flat plate.

Flow in an entrance region between parallel plates may be regarded as flat plate flow with the added effect of accelerated free stream velocity. An estimate of the increase in free stream velocity may be obtained by imposing the condition of continuity for the control volume shown below:

$$V_o h = \int_0^h v_x \, dy \, . \tag{E1}$$

Section 2 downstream is the section where fully developed flow persists in the channel; the velocity distribution follows the 1/7 power law here and we may write:

$$V_o h = V_{max} \int_0^h \left(\frac{y}{h}\right)^{1/7} dy \, . \tag{E2}$$

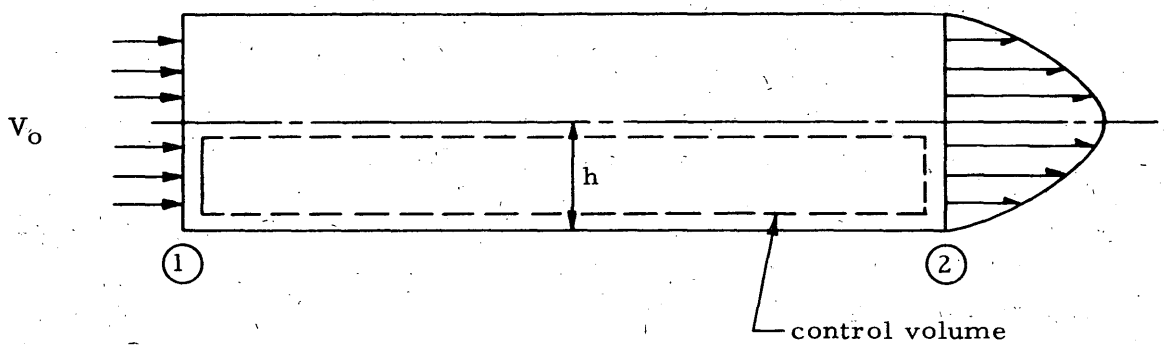

The integration may be carried out to obtain:

$$\frac{V_{max}}{V_o} = \frac{8}{7} = 1.143 \, . \tag{E3}$$

Hence the free stream velocity is accelerated 14.3% in the entrance region.

Since the free stream acceleration is small, we expect the 1/7 velocity distribution to hold for the entrance region. Adapted from pipe flow this becomes:

$$\frac{v_x}{V} = \left(\frac{y}{\delta}\right)^{1/7} \, . \tag{E4}$$

APPENDIX E

The momentum equation for entrance flow (Fig. E1) is:

$$-\frac{h}{\rho}\frac{dp}{dx} - \frac{\tau_w}{\rho} = 2V(h-\delta)\frac{dV}{dx} - V^2\frac{d\delta}{dx} - \frac{d}{dx}\int_0^\delta v_x^2\, dy. \qquad \text{(E5)}$$

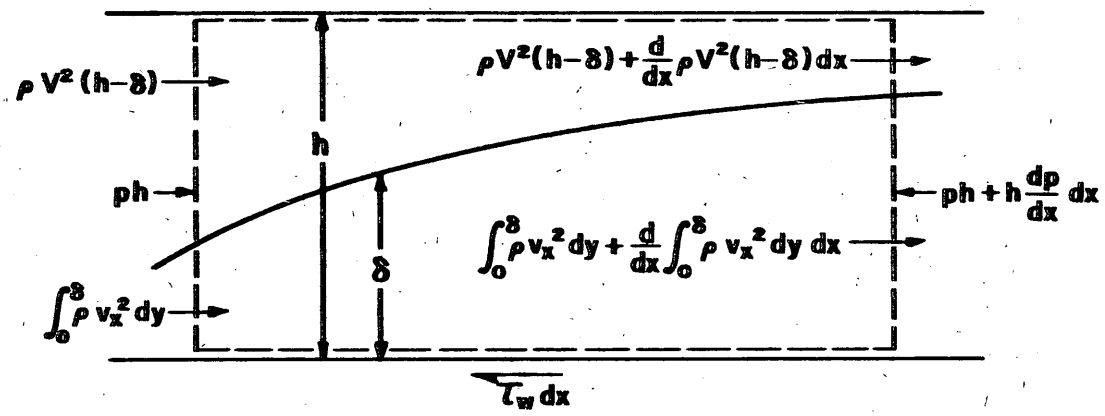

Figure E1. Entrance flow.

In the free stream the flow is frictionless and may be regarded as potential flow for which Euler's equation holds:

$$\frac{dp}{dx} = -\rho V\frac{dV}{dx}. \qquad \text{(E6)}$$

Inserting expressions E4 and E6 into eq E5 results in:

$$-\frac{\tau_w}{\rho} = hV\frac{dV}{dx} + \frac{4}{9}\delta V\frac{dV}{dx} - \frac{2}{9}V^2\frac{d\delta}{dx}. \qquad \text{(E7)}$$

The continuity equation for entrance flow may be written:

$$hV_o = \int_0^\delta v_x\, dy + (h-\delta)V. \qquad \text{(E8)}$$

When the velocity profile is inserted and the integration carried out we have:

$$V = \frac{V_o}{1-(\delta/8h)}. \qquad \text{(E9)}$$

Inserting eq E9 into eq E7 and carrying out the differentiation we obtain:

$$\frac{\tau_w}{\rho V^2} = \frac{\frac{1}{8h}}{(h-\frac{\delta}{8})}\frac{d\delta}{dx} - \frac{\frac{1}{18}\delta}{(h-\frac{\delta}{8})}\frac{d\delta}{dx} - \frac{2}{9}\frac{d\delta}{dx}. \qquad \text{(E10)}$$

The Blasius expression for friction is adapted for entrance flow in the same manner as for flat plate flow:

$$\left(\frac{\tau_w}{\rho V^2}\right) = 0.0233 \left(\frac{V\delta}{\nu}\right)^{-1/4} . \qquad \text{(E11)}$$

After considerable rearrangement, the following equation for boundary layer thickness is obtained:

$$\int_0^x \frac{1}{8h} (0.0233)\left(\frac{V_o h}{\nu}\right)^{-1/4} dx = \int_0^z \frac{8^{-3/4} z^{1/4}}{(1-z)^{5/4}} + \frac{\frac{8^{5/4}}{18} z^{5/4}}{(1-z)^{5/4}} + \frac{\frac{2}{9} 8^{1/4} z^{1/4}}{(1-z)^{1/4}} dz \qquad \text{(E12)}$$

where $z = \frac{\delta}{8h}$. This relation is integrated numerically to obtain the following expression for boundary layer thickness:

$$\frac{\delta}{h} = 0.353 \left[\frac{x}{h} \frac{V_o h}{\nu}^{-1/4}\right]^{0.749} . \qquad \text{(E13)}$$

The exponent is sufficiently close to 0.75 to be replaced by 3/4. We obtain for the correction to the flat plate equation for boundary layer thickness:

$$\frac{\delta}{h} = 0.353 \left(\frac{V_o h}{\nu}\right)^{-3/16} \left(\frac{x}{h}\right)^{15/16} . \qquad \text{(E14)}$$

Figure E2 shows boundary layer thickness and shear stress predicted by equations E14 and D7. It is apparent that, for turbulent flow, entrance effects do not significantly alter the boundary layer thickness and shear stress predicted by the flat plate formulas. It is clear, however, that eq E14 does not predict the correct asymptotic behavior of the boundary layer thickness as it approaches half the plate separation. This is because the solution of eq E14 was not obtained exactly, but it is surely valid for underdeveloped flow in the entrance region itself.

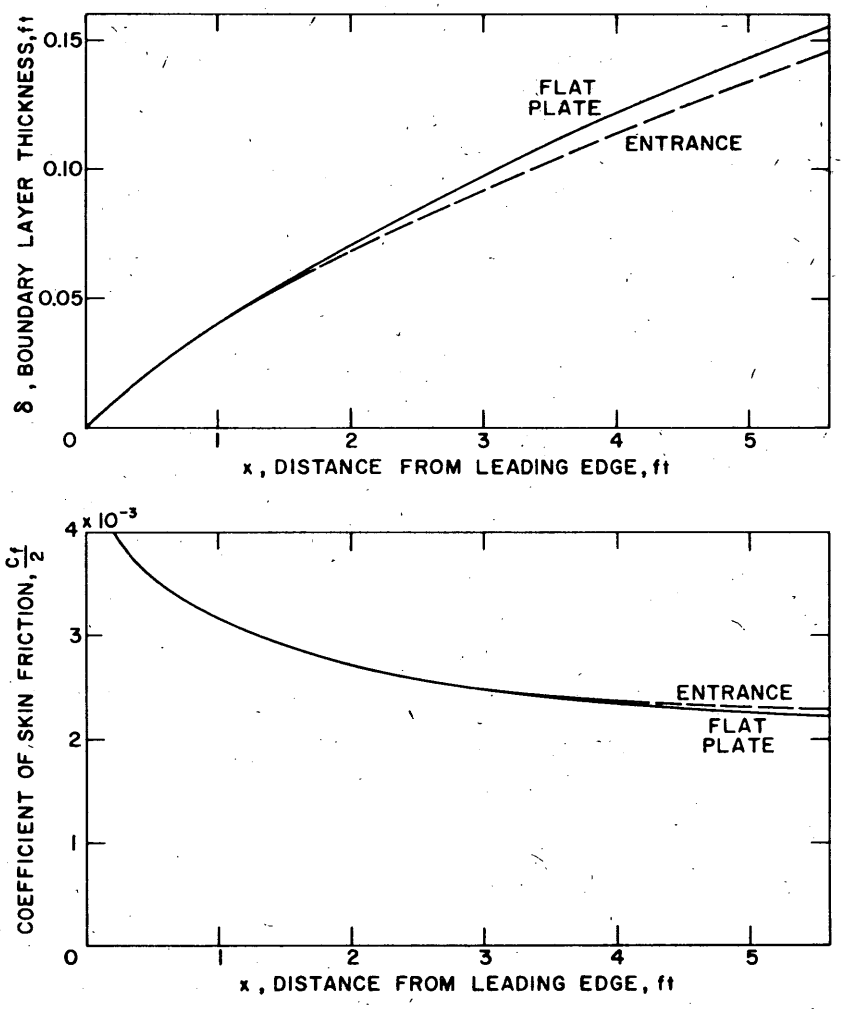

Figure E2. Comparison of flat plate and entrance formulas.

APPENDIX F. EFFECT OF NONISOTHERMAL SNOW SURFACE

Consider the heat transfer from a flat plate where the wall temperature is a step function as shown below:

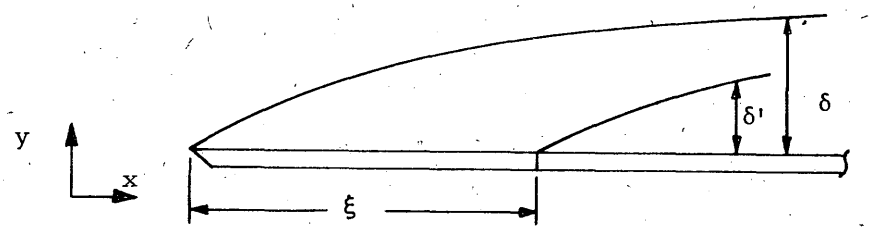

$$\theta = \frac{T - T_s}{T_a - T_s} = 1 \qquad x \leq \xi$$

$$\theta = 1 \qquad x > \xi,\ y = \infty$$

$$\theta = 0 \qquad x > \xi,\ y = 0$$

Rubesin [1951] first derived the relation for the heat transfer coefficient in terms of the unheated starting length ξ, for steady, two-dimensional, incompressible, turbulent flow over the plate. A somewhat more rigorous derivation is given by Reynolds, Kays, and Kline [1957], although their result does not differ significantly from the result obtained by Rubesin. According to Reynolds, Kays, and Kline:

$$h(x, \xi) = h_T(x) \left(1 - \left(\frac{x}{\xi}\right)^{9/10}\right)^{-1/9} \quad \text{for } x > \xi \qquad \text{(F1)}$$

where $h_T(x)$ is the isothermal heat transfer coefficient given by the Colburn modification of the Reynolds analogy (eq 21).

Tribus and Klein [1953] have shown how the heat transfer coefficient may be calculated from a surface with an arbitrary wall temperature distribution. For the present case of flat plate heat transfer, this is accomplished by forming the integral over an infinitely large number of steps in wall temperature:

$$\frac{q}{A} = \int_0^x h_T(x) \left(1 - \left(\frac{x}{\xi}\right)^{9/10}\right)^{-1/9} dT_s(\xi) \qquad \text{(F2)}$$

where the integral must be taken in the Stieltjes sense.

It can be shown that the analogy between heat and mass transfer requires that the mass transfer obey similar relations. The mass transfer from a flat plate with arbitrary wall temperature is:

$$\frac{g}{A} = \int_0^x \rho h_D(x) \left(1 - \left(\frac{x}{\xi}\right)^{9/10}\right)^{-1/9} dH_s(\xi) \qquad \text{(F3)}$$

where $h_D(x)$ is the mass transfer coefficient given by the Colburn analogy (eq 18).

To obtain an estimate of the importance of nonisothermal effects, assume that the humidity ratio $H_s(\xi)$ rises along the plate according to:

$$H_s(\xi) - H_a = C_1 \xi^{1/2} \tag{F4}$$

where the constant C_1 has dimensions $(\text{length})^{-1/2}$. The derivative in eq F3 is:

$$\frac{dH_s(\xi)}{d} = \frac{d(H_s(\xi) - H_a(\xi))}{d\xi} = \frac{C_1}{2} \xi^{-1/2} . \tag{F5}$$

This relation may be substituted into eq F3; carrying out the integration we obtain:

$$\frac{g}{A} = \rho h_D(x) \frac{C_1}{2} \frac{10}{9} x^{1/2} \frac{\Gamma(\frac{8}{9}) \Gamma(\frac{5}{9})}{\Gamma(\frac{13}{9})} . \tag{F6}$$

Since the mass transfer coefficient is defined by:

$$\rho h_D = \frac{g/A}{H_s(x) - H_a}$$

we may write:

$$h_D(x) = h_D(x) \frac{\frac{5}{9} \Gamma(\frac{8}{9}) \Gamma(\frac{5}{9})}{\Gamma(\frac{13}{9})} = 1.111 \, h_D(x) \tag{F7}$$

Thus the mass transfer coefficient is increased by 11.1% due to a 1/2 power law increasing humidity ratio at the surface. It can be shown that, as the power assumed in eq F4 is decreased, the percentage of increase in the mass transfer coefficient is increased by only 4%. Since the humidity ratio increase for the snow surface is well below a 1/2 power law for the range of temperature and energy transfers considered, the nonisothermal effects may be assumed to be negligible.

APPENDIX G. COMPUTER PROGRAM AND RESULTS FOR SUBLIMATION FROM THE UNIFORMLY HEATED SNOW SURFACE

Equation 31 is solved numerically by iteration for various values of Q/h_c, $T_a - T_{dp}$, and the temperature level T_a. The calculations were done by the GE-235 computer at Dartmouth College. The computer program is in "Basic"; the language is written by the Mathematics Department of Dartmouth College.

The results of program I are presented in tabular form. TA is the air temperature, TA-TDP represents the difference between the air temperature and the dewpoint temperature of the air, and Q/HC is the ratio of the energy input to the snow and the heat transfer coefficient. Values of the snow temperature difference ($T_s - T_a$) have been calculated for four values of ($T_a - T_{dp}$), 25 values of Q/h_c, and 9 values of T_a.

Program II solves eq 31 and uses eq 24 and 25 to obtain the mass transfer (g/A) as a function of distance from the leading edge (x) for the given values of Q = 25 Btu/hr-ft^2, V = 10 ft/sec, and T_a = 0F. The dependence of mass transfer rate is seen to change as the dewpoint temperature is raised from a very low value to the air temperature.

Program I - Solution to Eq 31

```
  5 DIM G(360), Q(25), T(4)
  6 FOR I=1TO25
  7 READ Q(I)
  8 NEXT I
 10 LET T=-25
 20 FOR K=1TO9
 35 LET T=T+5
 38 PRINT "TA="T
 39 PRINT
 40 PRINT
 45 LET T(1)=50
 46 LET T(2)=10
 47 LET T(3)=5
 48 LET T(4)=0
 49 PRINT "TA-TDP=", T(1), T(2), T(3), T(4)
 50 PRINT
 51 PRINT "Q/HC", "TS-TA", "TS-TA", "TS-TA", "TS-TA"
110 LET B=-160
112 FOR I=1TO360
113 LET B=B+1
115 LET A=5/9*(B-32)+273.1
120 LET H=-2445.5646/A+8.2312/2.30259*LOG(A)-.01677006*A
130 LET H=H+1.20514*10↑(-5)*A↑2-6.757169
140 LET H=10↑H
150 LET G(I)=18.015/28.95*H/(760-H)
160 NEXT I
161 FOR J=1TO25
162 LET Q=Q(J)
163 PRINT Q,
165 FOR I=1TO4
166 LET T1=T-T(I)
167 LET T2=T(I)
170 LET A=T1
180 GO SUB 300
190 LET H1=H
230 LET T3=T+1
240 LET A=T3
250 GO SUB 300
260 LET H3=H
270 LET A=Q-T2*1.112/.239*1220*(H3-H1)/(T3-T1)
280 LET T4=A/(1+1.112*1220/.239*(H3-H1)/(T3-T1))+T
285 IF ABS(T4-T3)<.002 THEN 330
290 LET T3=(T4+T3)/2
295 GO TO 240
300 LET A=A+160
302 IF A>200 THEN 345
303 IF A<1 THEN 345
305 LET A1=A-INT(A)
310 LET M=INT(A)
315 LET H=G(M)+A1*(G(M+1)-G(M))
320 RETURN
330 LET T5=T3-T
340 PRINT T5,
345 NEXT I
350 NEXT J
360 NEXT K
365 DATA .05, .1, .5, 1, 2, 4, 6, 8, 10, 12, 14, 16, 18, 20, 25, 30, 35, 40, 45, 50, 55
366 DATA 60, 65, 70, 75
370 END
```

Results of Program I

$T_a - T_{dp}$ and $T_s - T_a$ in °F

TA=-20

TA-TDP=	50	10	5	0
Q/HC	TS-TA	TS-TA	TS-TA	TS-TA
.05	-1.27618	-.563258	-.298959	4.78316 E-2
.1	-1.22986	-.517136	-.252842	.09371
.5	-.859919	-.147186	.116391	.460738
1	-.397707	.312315	.576039	.920625
2	.522819	1.22802	1.49002	1.83351
4	2.35143	3.05376	3.31319	3.65408
6	4.16755	4.8636	5.12128	5.45774
8	5.96805	6.65606	6.91265	7.24611
10	7.74997	8.43247	8.6852	9.01609
12	9.5141	10.1899	10.4395	10.7664
14	11.2597	11.928	12.1748	12.4973
16	12.9857	13.645	13.8896	14.2084
18	14.6899	15.3416	15.5825	15.899
20	16.3731	17.0172	17.2543	17.5657
25	20.4818	21.1031	21.3318	21.6313
30	24.4403	25.0379	25.2575	25.545
35	28.2405	28.8121	29.024	29.2986
40	31.876	32.421	32.6235	32.8876
45	35.345	35.8658	36.0583	36.3077
50	38.6483	39.1437	39.3256	39.5637
55	41.7879	42.2574	42.4302	42.6576

TA=-15

TA-TDP=	50	10	5	0
Q/HC	TS-TA	TS-TA	TS-TA	TS-TA
.05	-1.66729	-.732568	-.394172	.04676
.1	-1.62196	-.687477	-.349085	9.15668 E-2
.5	-1.25936	-.326752	1.23759 E-2	.450021
1	-.806088	.124192	.46152	.899486
2	9.49748 E-2	1.01945	1.35439	1.79003
4	1.88327	2.80101	3.13301	3.56454
6	3.65711	4.56486	4.89379	5.31984
8	5.41137	6.30946	6.63414	7.05746
10	7.14785	8.03575	8.35612	8.77296
12	8.8628	9.73928	10.0569	10.4675
14	10.5561	11.4216	11.7347	12.141
16	12.2282	13.0825	13.3904	13.791
18	13.8776	14.719	15.024	15.4176
20	15.5027	16.3322	16.6318	17.0215
25	19.4602	20.2577	20.5453	20.9195
30	23.2595	24.0242	24.2988	24.656
35	26.8943	27.6228	27.8878	28.2285
40	30.3623	31.0585	31.3079	31.6325
45	33.6638	34.3257	34.5638	34.8737
50	36.8036	37.4304	37.6567	37.9525
55	39.7836	40.3785	40.5931	40.8724

TA=-10

TA-TDP=	50	10	5	0
Q/HC	TS-TA	TS-TA	TS-TA	TS-TA
.05	-2.14885	-.937122	-.508871	4.54764 E-2
.1	-2.10447	-.89327	-.465024	8.89996
.5	-1.75086	-.542457	-.113278	.437186
1	-1.30954	-.10308	.322731	.874166
2	-.429722	.769522	1.1912	1.7381
4	1.31281	2.49812	2.91772	3.45818
6	3.03815	4.20928	4.62305	5.15698
8	4.74215	5.89862	6.30683	6.83468
10	6.4242	7.56501	7.97003	8.48861
12	8.08485	9.20955	9.60774	10.1204
14	9.72223	10.9313	11.2229	11.7272
16	11.3354	12.4274	12.8135	13.3098
18	12.9249	14.0004	14.3788	14.868
20	14.4879	15.5456	15.9199	16.3995
25	18.2851	19.299	19.6563	20.1169
30	21.9198	22.8871	23.2286	23.6672
35	25.3863	26.3082	26.6328	27.0529
40	28.6868	29.564	29.8739	30.2703
45	31.8254	32.6569	32.9526	33.3282
50	34.8043	35.5933	35.8726	36.2296
55	37.6291	38.3778	38.6427	38.9839

TA=-5

TA-TDP=	50	10	5	0
Q/HC	TS-TA	TS-TA	TS-TA	TS-TA
.05	-2.73427	-1.18133	-.644718	4.39652 E-2
.1	-2.69125	-1.13864	-.602336	8.59773 E-2
.5	-2.34713	-.7986	-.263287	.422074
1	-1.91761	-.374732	.159965	.843121
2	-1.06251	.470575	1	1.67713
4	.629546	2.1411	2.66433	3.33311
6	2.29757	3.79109	4.30751	4.96785
8	3.94652	5.41816	5.92712	6.57707
10	5.57097	7.0218	7.52111	8.16255
12	7.17183	8.59871	9.09306	9.72216
14	8.74729	10.1522	10.6372	11.2568
16	10.2978	11.679	12.157	12.7655
18	11.8231	13.1809	13.6496	14.248
20	13.3217	14.6556	15.1173	15.704
25	16.955	18.228	18.6674	19.2281
30	20.4195	21.6331	22.0523	22.585
35	23.7185	24.8741	25.2706	25.7775
40	26.8556	27.9518	28.3283	28.81
45	29.8329	30.8727	31.2298	31.6867
50	32.6561	33.6428	33.9841	34.4147
55	35.3352	36.2705	36.5916	37.0057

TA=0

TA-TDP=	50	10	5	0
Q/HC	TS-TA	TS-TA	TS-TA	TS-TA
.05	-3.43455	-1.46738	-.802678	.042219
.1	-3.3928	-1.42634	-.761996	8.24849 E-2
.5	-3.05881	-1.09799	-.43654	.404612
1	-2.64426	-.690326	-2.88965 E-2	.808402
2	-1.81672	.122854	.778088	1.60691
4	-.181175	1.7267	2.37276	3.19126
6	1.42767	3.31006	3.94636	4.75107
8	3.01647	4.86859	5.49238	6.28472
10	4.57727	6.39987	7.01513	7.79391
12	6.11474	7.90683	8.50926	8.27567
14	7.62596	9.38593	9.97984	10.7312
16	9.1174	10.8401	11.4213	12.1607
18	10.5694	12.2668	12.8382	13.5623
20	12.003	13.6669	14.2275	14.9392
25	15.4639	17.0526	17.5844	18.2613
30	18.7619	20.2708	20.7778	21.419
35	21.8968	23.3276	23.8102	24.4186
40	24.871	26.23	26.6859	27.265
45	27.693	28.9842	29.4149	29.9648
50	30.37	31.5919	32.0058	32.5231
55	32.9102	34.0707	34.4583	34.9547

TA=5

TA-TDP=	50	10	5	0
Q/HC	TS-TA	TS-TA	TS-TA	TS-TA
.05	-4.2592	-1.79538	-.982753	4.02413 E-2
.1	-4.21887	-1.75622	-.944003	7.85294
.5	-3.89723	-1.44295	-.634009	.384834
1	-3.49765	-1.0514	-.24653	.769079
2	-2.7005	-.274979	.523889	1.52669
4	-1.12695	1.25667	2.04334	3.03229
6	.421242	2.76588	3.53719	4.50918
8	1.94329	4.24782	5.008	5.96149
10	3.43822	5.70433	6.44861	7.3848
12	4.9105	7.13436	7.86498	8.78421
14	6.35358	8.53622	9.25347	10.1559
16	7.77128	9.91351	10.6154	11.4998
18	9.16239	11.2623	11.9525	12.8188
20	10.5257	12.5849	13.2608	14.1112
25	13.8208	15.7781	16.4194	17.2261
30	16.9527	18.8094	19.4189	20.1847
35	19.9241	21.6862	22.2642	22.9925
40	22.7432	24.4151	24.8651	25.6522
45	25.4173	27.0059	27.5233	P 28.1772
50	27.9555	29.4584	29.9548	30.5723
55	30.3612	31.7907	32.2589	32.859

TA=10

TA-TDP=	50	10	5	0
Q/HC	TS-TA	TS-TA	TS-TA	TS-TA
.05	-5.21615	-2.16658	-1.18586	3.80485 E-2
.1	-5.17739	-2.12909	-1.14883	7.41438 E-2
.5	-4.86872	-1.83029	-.854385	.362907
1	-4.48515	-1.4598	-.488427	.7244
2	-3.72021	-.72233	.24095	1.43933
4	-2.21229	.733703	1.67581	2.85605
6	-.730211	2.16063	3.08889	4.2452
8		3.5623	4.47186	5.60696
10	2.15256	4.93886	5.83143	6.94397
12	3.55461	6.28664	7.16289	8.25235
14	4.9313	7.60967	8.467	9.53495
16	6.27937	8.90692	9.74626	10.7938
18	7.60266	10.1765	11.0007	12.0255
20	8.90008	11.4198	12.2266	13.2303
25	12.0268	14.4182	15.1851	16.1378
30	14.9957	17.2646	17.9928	18.8963
35	17.8108	19.9653	20.6515	21.5091
40	20.4809	22.5234	23.1775	23.9926
45	23.0164	24.954	25.5725	26.3445
50	25.4184	27.2591	27.8482	28.5811
55	27.7009	29.4499	60	

TA=15

TA-TDP=	50	10	5	0
Q/HC	TS-TA	TS-TA	TS-TA	TS-TA
.05	-6.31006	-2.57712	-1.40871	3.56708 E-2
.1	-6.27299	-2.5419	-1.37398	6.93885 E-2
.5	-5.97685	-2.26011	-1.09616	.33913
1	-5.61068	-1.90836	-.752436	.676941
2	-4.879	-1.21359	-6.66529 E-2	1.34497
4	-3.4401	.15862	1.27839	2.6662
6	-2.02446	1.49971	2.60041	3.9629
8	-.639773	2.81819	3.89824	5.23042
10	.720788	4.11106	5.16771	6.4726
12	2.05396	5.37554	6.41195	7.69019
14	3.36011	6.61534	7.63064	8.88334
16	4.64092	7.83054	8.82488	10.0514
18	5.89695	9.02103	9.99483	11.1936
20	7.12621	10.1846	11.1383	12.3123
25	10.0899	12.9922	13.8957	15.011
30	12.9011	15.6519	16.5084	17.5665
35	15.5651	18.1777	18.9919	19.9961
40	18.0963	20.5717	21.3447	22.2974

TA=20

TA-TDP=	50	10	5	0
Q/HC	TS-TA	TS-TA	TS-TA	TS-TA
.05	-7.54152	-3.01988	-1.64842	3.31512 E-2
.1	-7.50629	-2.98687	-1.61615	6.43493 E-2
.5	-7.22446	-2.72462	-1.35706	.313934
1	-6.87398	-2.39681	-1.03452	.626647
2	-6.17798	-1.74454	-.399012	1.24448
4	-4.80789	-.461761	.858599	2.46668
6	-3.46481	.795534	2.0862	3.66304
8	-2.14587	2.02548	3.29005	4.83656
10	-.854329	3.23049	4.4691	5.98508
12	.409618	4.41156	5.62418	7.10796
14	1.64693	5.56781	6.7566	8.20732
16	2.86187	6.70031	7.86462	9.28392
18	4.05101	7.80936	8.94949	10.3382
20	5.21378	8.89529	10.0114	11.3705
25	8.01986	11.5089	12.5658	13.8596
30	10.6782	13.9923	14.9954	16.2207
35	13.2025	16.3449	17.2977	18.4627

Program II - Mass Transfer Rate

```
  5 DIM G(360)
  6 LET T=0
  7 LET R=25
 10 PRINT "TA=0 F VEL=10 FT/SEC Q=25 BTU/HR-FT2"
 15 PRINT
 16 PRINT
 17 PRINT "TA-TDP=", "35", "30", "25", "20"
 18 PRINT
 19 PRINT "X-FT", "MASS-TR", "MASS-TR", "MASS-TR", "MASS-TR"
110 LET B=-160
112 FOR I=1TO360
113 LET B=B+1
115 LET A=5/9*(B-32)+273.1
120 LET H=-2445.5646/A+8.2312/2.30259*LOG(A)-.01677006*A
130 LET H=H+1.20514*10↑(-5)*A↑2-6.757169
140 LET H=10↑H
150 LET G(I)=18.015/28.95*H/(760-H)
160 NEXT I
161 LET X=0
162 FOR J=1TO10
163 LET X=X+10
164 LET Q=R/(.0863*.239*36000↑.8*(.463/X)↑.2*.0376)
165 PRINT X,
166 LET T1=T-40
167 FOR I=1TO4
168 LET T1=T1+5
169 LET T2=T-T1
170 LET A=T1
180 GO SUB 300
190 LET H1=H
230 LET T3=T+1
240 LET A=T3
250 GO SUB 300
260 LET H3=H
270 LET A=Q-T2*1.112/.239*1220*(H3-H1)/(T3-T1)
280 LET T4=A/(1+1.112*1220/.239*(H3-H1)/(T3-T1))+T
285 IF ABS(T4-T3)<.002 THEN 330
290 LET T3=(T4+T3)/2
295 GO TO 240
300 LET A=A+160
302 IF A>200 THEN 345
303 IF A< THEN 345
305 LET A1=A-INT(A)
310 LET M=INT(A)
315 LET H=G(M)+A1*(G(M+1)-G(M))
320 RETURN
330 LET S=1.112/.239/Q*25*(H3-H1)
340 PRINT S,
341 NEXT I
342 NEXT J
345 END
```

Results of Program II

TA=0 F VEL=10 FT/SEC Q=25 BTU/HR-FT2

TA-TDP=	35	30	25	20
X-FT	MASS-TR	MASS-TR	MASS-TR	MASS-TR
10	9.05612 E-3	8.80854 E-3	8.48215 E-3	8.05811 E-3
20	8.56289 E-3	8.35247 E-3	8.07504 E-3	7.71221 E-3
30	8.32296 E-3	8.13109 E-3	7.87844 E-3	7.54805 E-3
40	8.17437 E-3	7.99343 E-3	7.75592 E-3	7.44802 E-3
50	8.06915 E-3	7.89833 E-3	7.67312 E-3	7.37866 E-3
60	7.99001 E-3	7.82529 E-3	7.61015 E-3	7.32998 E-3
70	7.92822 E-3	7.77061 E-3	7.56283 E-3	7.291Q7 E-3
80	7.87877 E-3	7.72531 E-3	7.52299 E-3	7.26136 E-3
90	7.83622 E-3	7.68751 E-3	7.49259 E-3	7.23775 E-3
100	7.80226 E-3	7.65748 E-3	7.46661 E-3	7.21709 E-3

TA=0 F VEL=10 FT/SEC Q=25 BTU/HR-FT2

TA-TDP=	15	10	5	0
X-FT	MASS-TR	MASS-TR	MASS-TR	MASS-TR
10	7.50902 E-3	6.79851 E-3	5.89564 E-3	4.74909 E-3
20	7.23993 E-3	6.63119 E-3	5.86109 E-3	4.88205 E-3
30	7.11758 E-3	6.56756 E-3	5.86091 E-3	4.97009 E-3
40	7.04682 E-3	6.52999 E-3	5.87161 E-3	5.03736 E-3
50	6.99881 E-3	6.50910 E-3	5.88362 E-3	5.09015 E-3
60	6.96489 E-3	6.49550 E-3	5.89661 E-3	5.13862 E-3
70	6.93961 E-3	6.48795 E-3	5.90977 E-3	5.17827 E-3
80	6.92135 E-3	6.48159 E-3	5.92387 E-3	5.21530 E-3
90	6.90565 E-3	6.48057 E-3	5.93599 E-3	5.24860 E-3
100	6.89454 E-3	6.47983 E-3	5.94912 E-3	5.27772 E-3

APPENDIX H. COMPUTER PROGRAM AND RESULTS FOR THE NETWORK ANALYSIS

The computer program which solves the thermal network presented in section IV and Appendix B is presented here. This analysis accounts for the nonisothermal character of the radiation to the snow surface. The simpler network which assumes the radiant interchange to take place from isothermal surfaces is a special case of this analysis and therefore is not included here. This analysis corresponds to the solid lines of Figures 3 and 4.

Program III - Computer Program for Nonisothermal Network

```
  4 DIM X(23), P(12), Q(12)
  5 DIM C(11), G(260), R(12), H(12), A(23), B;VJ
 10 FOR I=1TO11
 15 READ C(I)
 20 NEXT I
 25 DATA .1045E-2, .241E-2, .6847E-2, .2714E-1, .1566
 30 DATA .39, .1566, .2741E-1, .6847E-2, .241E-2, .1045E-2
 35 LET A=-60
 40 FOR I=1TO260
 45 LET A=A+1
 50 LET B=5/9*(A-32)+273.1
 55 LET C=2445.5646/B+8.2312/2.30259*LOG(B)-.01677006*B
 60 LET C=C+1.20514E-5*B 2-6.757169
 65 LET C=10↑C
 70 LET G(I)=18.015/28.95*C/(760-C)
 71 NEXT I
 75 LET T=3
 80 LET Q=248
 85 LET V=8.5
 90 LET T5=-6.5
 95 PRINT
100 PRINT
105 PRINT "TA="T, "VEL="V, "Q, "TDP="T5
110 PRINT
115 PRINT "X", "TP", "DEL TS", "MASS TR"
120 PRINT
125 LET A=T5+60
130 LET H1=G(INT(A))+(A-INT(A))*(G(INT(A)+1)-G(INT)(A)))
135 LET T2=T
140 LET T3=T
145 LET S=1
150 FOR K=1TO12
155 LET S=S+.5
160 LET A=T3+60
165 LET H3=G(INT(A))+(A-INT(A))*(G(INT(A)+1)-G(INT(A)))
170 LET R(K)=1.26*.0296*(V*S*3600/.46)↑(-1/5*V*3600*.086*.239
175 LET R2=.585*.1713E-8*(T2+T3+920)*(T2+460)↑2+(T3+460)↑2)
180 LET R3=1220*R(K)*(H3-H1)/.239/(T3-T5)*1.11
185 LET H(K)=R(K)*(1-(1/S)↑(9/10))↑(-1/9)
190 LET A=(R3*T5+R(K)*(R2+H(K))+R2*(Q-H(K)*T)
195 LET B=(R(K)+R2+R3)*(R2+H(K))-R2↑2
200 LET C=(R(K)+R2+R3)*(Q-H(K)*T)+R2*(R3*T5+R(K)*T)
205 LET T6=A/B
210 LET T2=C/B
215 IF ABS((T6-T3)/2)<.002 THEN 230
220 LET T3=(T6+T3)/2
225 GO TO 160
230 LET A(K+6)=T2
235 LET B(K+6)=T3
237 GO SUB 510
240 NEXT K
245 FOR I=2TO5
250 LET A(I)=T
255 LET B(I)=T
260 NEXT I
265 FOR I=19TO23
270 LET A(I)=A(18)
275 LET B(I)=B(18)
280 NEXT I
285 LET A(6)=(T+A(7))/2
290 LET B(6)=(T+B(7))/2
295 FOR I=7TO18
300 LET X(I)=0
305 LET N=0
310 FOR J=I-5TOI+5
315 LET N=N+1
320 LET X(I)=1/3.7781*C(N)*.1713E-8*(B(J)+460)↑4+X(I)
325 NEXT J
330 LET X(I)=X(I)+1/3.7781*3*.1713E-8*(A(I)+460)↑4
335 NEXT I
340 FOR I=2TO5
345 LET X(I)=.1713E-8*(T+460)↑4
350 NEXT I
355 FOR I=19TO23
360 LET X(I)=X(18)
365 NEXT I
370 LET X(6)=(X(7)+X(5))/2
375 FOR I=7TO18
380 LET N=0
385 LET P(I-6)=0
390 LET Q(I-6)=0
395 FOR J=I-5TOI+5
400 LET N=N+1
405 LET P(I-6)=P(I-6)+C(N)*(X(I)-.1713E-8*(B(J)+460)↑4)
410 LET Q(I-6)=Q(I-6)+C(N)*(X(J)-.1713E-8*(B(I)+460)↑4)
415 NEXT J
420 NEXT I
```

Program III (Cont'd)

```
425 LET S=1
430 FOR K=1TO12
440 LET S=S+.5
445 LET T4=(Q-P(K)+(H(K)+.124)*T)/(H(K)+.124)
446 LET T2=(T4+A(K+6))/2
450 LET T3=B(K+6)
455 LET A=T3+60
460 LET H3=G(INT(A))+(A-INT(A))*(G(INT(A)+1)-G(INT(A)))
465 LET R3=1220*R(K)*(H3-H1)/.239/(T3-T5)*1.11
470 LET T6=(Q(K)+T*(R(K)+.14)+T5*R3)/(R(K)+R3+.14)
475 IF ABS(T6-T3)<.002THEN490
480 LET T3=(T3+T6)/2
485 GO TO 455
490 LET A(K+6)=T2
495 LET B(K+6)=T3
497 GO SUB 510
500 NEXT K
505 GO TO 245
510 LET T8=T3-T
515 LET S1=(T3-T5)*R3/1220
520 PRINT S, T2, T8, S1
525 RETURN
530 END
```

Results of Program III

TA=3	VEL= 8.5	Q= 248	TDP= -6.5
X	TP	DEL TS	MASS TR
1.5	78.3602	8.30888	9.20729 E-3
2	84.9219	10.8294	1.06133 E-2
2.5	89.2633	12.3171	1.13392 E-2
3	92.5658	13.4444	.011854
3.5	95.254	14.3796	1.22692 E-2
4	97.5307	15.1897	1.26241 E-2
4.5	99.5104	15.9095	1.29391 E-2
5	101.265	16.5608	1.32298 E-2
5.5	102.842	17.1589	1.34941 E-2
6	104.273	17.7095	1.37416 E-2
6.5	105.581	18.2116	1.39627 E-2
7	106.77	18.6256	1.41232 E-2

TA=21.5	VEL= 8.5	Q= 88.4	TDP= 10
X	TP	DEL TS	MASS TR
1.5	48.1661	-.255012	.010526
2	50.5098	.485219	1.07781 E-2
2.5	52.0931	.921118	1.08015 E-2
3	53.3096	1.25591	.010781
3.5	54.3065	1.53738	.010754
4	55.1551	1.78029	1.07327 E-2
4.5	55.8963	1.99789	1.07121 E-2
5	56.5556	2.19588	.010693
5.5	57.1502	2.37959	1.06771 E-2
6	57.6918	2.54925	1.06638 E-2
6.5	58.1881	2.70354	1.06522 E-2
7	58.6412	2.83353	1.06265 E-2